Norwegian University
of Life Sciences

Master's Thesis 2018   30 ECTS

Changes in crown form by mixing Norway spruce and Scots pine analysed with terrestrial laser scanning

Kine Fliflet

Forest Sciences
Faculty of Environmental Sciences and Natural Resource Management

Acknowledgments

II

Abstract

How tree´s crown form develops in mixed stands are of interest, especially due to the linkage between light interception and biomass production. There are some studies revealing development of greater crown forms (e.g., crown radius, crown length or crown volume) in mixed forests. This paper addresses how individual trees of Norway spruce (*Picea abies* (L.) Karst.) and Scots pine (*Pinus sylvestris* L.) change their crown form when growing in a mixture, compared to them growing and competing with neighbors of the same species. To quantify if there is a change in crown form in mixtures, terrestrial laser scanning (TLS) have been used to obtain individual tree crown information in six stands and 24 plots containing a various species proportion of both spruce and pine. Crown form variables such as *maximum crown radius*, *crown length from tree height to height of maximum crown radius*, *crown volume above maximum crown radius* were used in a multiple linear regression analysis to test for whether there is a mixture effect in spruce. This was also done for pine, in addition to the crown variables *crown length from tree height to height of live-crown base* and *crown volume above live-crown base*. This study reveals a significant mixture effect on all crown form variables in spruce. In pine however, none of the crown form variables had a significant mixture effect.

IV

Sammendrag

Hvordan trekronen former og utvikler seg i blandede bestand er et interessant tema, spesielt fordi det er en sammenheng mellom trærs lysabsorpsjon og biomasseproduksjon. Det eksistere studier som viser til at trær i blandingsskoger utvikler større kroneform (i form av økt kroneradius, kronelengde eller kronevolum) sammenlignet med homogen skog. Denne oppgaven ser på hvordan individuelle trær av gran (*Picea abies* (L.) Karst.) og furu (*Pinus sylvestris* L.) endrer sin kroneform når de vokser i blanding, sammenlignet med når de vokser og konkurrerer med trær av samme treslag. For å kvantifisere denne effekten har informasjon fra individuelle trærs kroneform blitt samlet inn ved hjelp av bakkebasert laserskanning (TLS) hos 24 plot fordelt på seks bestand som alle inneholdt en variasjon i treslagsfordeling av furu og gran. Kronevariable som *maksimal kroneradius*, *kronelengde fra trehøyde til høyden til maksimal kroneradius* og *kronevolum fra maksimal kroneradius til trehøyde* ble brukt i en multippel lineær regresjonsanalyse for å teste hvorvidt det er en blandingseffekt i gran. Disse kronevariablene ble også brukt for å teste blandingseffekt i furu, i tillegg til variablene *kronelengde fra trehøyde til kronebasis* og *kronevolum over kronebasis til trehøyde*. Denne studien viser at det var en signifikant blandingseffekt hos alle kronevariable i gran. Hos furu derimot, var blandingseffekten ikke-signifikant hos alle kronevariablene analysert i denne oppgaven.

Table of contents

1. Introduction

Many of the world's forests consists of mixtures of multiple species which have potential benefits over monocultures. Some scientific literature has proven mixed-species forests to provide important ecosystem functions as well as increased production and economic outcomes (Gamfeldt et al. 2013; Griess & Knoke 2011; Pretzsch et al. 2015), resulting in increased habitats for biodiversity, increased recreational values, and/or increased growth rates (Felton et al. 2016; Paquette & Messier 2011). On the other hand, there is also evidence of mixed stands not providing additional benefits, hence resulting in decreased production and economic outcomes (Forrester 2014). The potential benefit or potential loss from mixed-species forests will for example vary with what kind of species are interacting, resource availability and climate conditions on site (Forrester & Bauhus 2016).

A tree's crown is the appuratus providing production of sugar components needed for the trees to grow and to maintain its structures. They are formed during the growth process of each individual tree, in addition to being influenced by individual trees in the nearby surroundings (Stenberg et al. 1994). Although different tree species develop different typical crown forms, which for example ranges from conical to more oval, umbrella-formed or even flat-topped, these forms vary because of the environment conditions affecting the crown structure of each individual tree (Pretzsch 2017).

The crown consists of foliage and branches growing from a trees trunk, and this silhouette defines a trees crown form. Trees change their crown form primarily through height growth, branch growth and/or crown recession (Iwasa et al. 1985). Height growth improves the crowns lighting condition and provides competitive advantages over surrounding trees. If crown base remains constant, crown length increases with height growth. Crown recession (shift in crown base, i.e, where the foliage ends) occurs when trees change their crown basis upwards. Trees cannot develop new crown below the crown basis. Crown basis will either remain constant or move upward as branches die at the crown base, normally because it can no longer hold up its foliage, mainly because of shading from neighboring trees. In dense stands, crowns recess with increasing height growth because of increased contact with neighboring trees, which decreases the light available in the lower canopy layers (Deleuze et al. 1996). Branch growth also declines with increasing competition from neighboring trees, but if available growing space occurs, for example from dying neighborhood trees, foliage may grow into the free space. The sum of growing and dying branches, in addition to varying

branching around stems, can create some asymmetries in crown form. Nonetheless, the tip of crown branches is a useful to describe a crowns radius, which together with crown length are used in calculating crowns volume. Altogether, the crown radius in multiple directions and crown length represents the crowns form. Individual trees crown form will change over time, and this change differs with stand density and what kind of species are present (Pretzsch 2017). This change and development of crown form is of interest, especially since there is a link between light interception and biomass production (Ford 1985; Stenberg et al. 1994). In that way, leaf area expresses resource acquisition on a site (Long et al. 2004). Larger crown forms in mixed-species forests might indicate increased leaf area in stands, which implies of a larger forest production within mixtures. For that reason are crowns an important object of research, in understanding the link between crown structure, light interception, and productivity in mixed-species forests compared to monocultures.

Trees ability to change their crown morphologically, either by height growth or branch growth, can be a plastic trait in terms of species responding within its generation to changes in the environment (Chambel et al. 2005; De Kort et al. 2016; Sorrensen-Cothern et al. 1993). This adaption ability varies between species, and can be calculated by estimating the means of a species reaction under different circumstances. The crowns diameter divided by diameter at breast height - ratio of trees growing under solitary conditions indicates the maximum crown extension (Pretzsch 2017). The same ratio for trees under fully stocked conditions indicates the minimum crown extension. These two metrics for a given diameter put in relation to each other provides information about the species relative potential for expansion. This was done by Pretzsch (2014), who introduces European beech (*Fagus sylvatica* L.) as one of the most plastic species, with the possibility to enlarge its crown 5.1 times more under solitary condition compared to under strong competition. European beech is followed by a 4.7 times enlargement for Silver fir (*Abies alba* Mill.), 4.5 for oak (*Quercus petraea* (Matt.) Liebl. and *Quercus robur* L.), 4.2 for Norway spruce (*Picea abies* (L.) Karst.), 3.7 for Scots pine (*Pinus sylvestris* L.) and 2.6 for Silver birch (*Betula pendula* Roth.). These calculations reveals that there is a difference between species in how much canopy space they have the potential to occupy. Mixing species with high plasticity may increase leaf area on site and thereby the production within mixed stands.

4

Some studies have proven mixed-species forests to exploit canopy space more efficient, in terms of increasing either crown length, crown radius or crown volume for trees growing in mixtures compared to monocultures (Barbeito et al. 2017; Jucker et al. 2015; Longuetaud et al. 2013). The idea is that tree species with complementary crown form might fully exploit the space available in the forest when growing in mixtures more efficiently. For example, by adapting their crowns trough height growth and/or widening their crown. This might increase light absorption in a forest and increase stand production (Forrester 2017). Jucker et al. (2015) found evidence of this optimization, although this research did not distinguish between which species were being mixed. Within stands, trees compete amongst each other in utilization of the resources available on site. In pure, homogeneous stands, trees compete with other trees with similar resource use, physiological abilities, and structural variability. As a result, canopy structure remains mostly homogenous due to this intra-specific competition (Pretzsch 2014). In mixed-species forests however, individual trees compete with trees with dissimilar resource use, physiological abilities, and structural variability, resulting in less competition between trees in for example light, because they have different shading tolerance and/or utilizing different parts of the canopy layers (Jucker et al. 2015) and/or have complementary root shape (Pretzsch 2017). Evidence of this change in crown form is for example found in mixtures of European beech and Scots pine, where mixtures caused denser canopy packing with longer crowns in beech (Barbeito et al. 2017; Pretzsch & Schutze 2005). There are also studies which implies that some mixtures even suppresses some species crown form, such as mixtures with Scots pine and European beech, where Scots pine developed smaller crowns in terms of width and length when growing in mixtures, compared to growing in pure stands (Forrester et al. 2018). This means that individual trees crown form might increase or decrease as a response to what kind of species are being their closest neighbor.

In Norway, Norway spruce and Scots pine in mixture occur frequently on sites of intermediate quality, but are rarely managed to maintain the mixture over time. Norway spruce and Scots pine have dissimilar morphological and physiological attributes in shade tolerance and drought tolerance. Norway spruce is a shade tolerant tree species, while Scots pine is more intolerant (Bauhus et al. 2017). There are reports of greater production benefits especially when trees with dissimilar traits grow in mixtures (Bauhus et al. 2017; Paquette & Messier 2011). But there are also results that indicate that these two species do not produce more in mixtures compared to pure stands (Lindén & Agestam 2003), most likely because they are not so different in their growth dynamics.

To quantify how trees growing in mixture exploit canopy space, terrestrial laser scanning (TLS) is useful. When using TLS, a laser beam deflects in millions of directions to scan a forest area (Hackenberg et al. 2014). When the laser beam hits an object, it reflects and travels back to the laser sensor. The fraction of light that returns to the scanner allows a distance to be computed by calculating the laser beams' travel time. The scanner creates a point with assigned X-, Y- and Z-coordinate for each reflection, which in total creates a point cloud of for example a forest stand. In due to millions of points that are recorded on the surface of each crown detail (such as branches, stem, or foliage), a 3D digitalization is made and provides detailed descriptions of individual trees that can be used for deriving tree information useful in analyzing crown structure and competitive conditions (Olivier et al. 2017; Seidel et al. 2015). The method has for example been used by Barbeito et al. (2017) who found higher live-crown ratios and greater crown expansion in European beech with the use of TLS, resulting in larger crown volumes when beech were growing in mixtures with Scots pine compared to pure stands. Also, Metz et al. (2013) used data derived from TLS to detect individual crown forms in forests in order to model the relationship between competition and growth. Measuring tree height, crown length and crown radius manually may not be as efficient nor providing accurate information about individual trees crown form variables. Terrestrial laser scanning on the other hand is an option for deriving more detailed crown information efficiently.

Since individual trees growing in mixtures are more likely to grow under less competition, the assumption is that this also applies in mixtures of Scots pine and Norway spruce. Especially since there are indications of tree species with dissimilar light ecology having larger effect of mixture. Less competition because of mixtures within a stand might increase individuals tree crown form. The hypothesis in this study is based on the idea that if individual pine trees are growing with spruce between them, and spruce are occupying canopy space in a different way than pine, this will result in pines to widen their crown. The objective of this study is to describe how Norway spruce and Scots pine change their crown radius, crown length and crown volume when growing in mixtures compared to pure stands. I hypothesize that there is a mixture effect in both species, specially that spruce trees, as a shade-tolerant species, may develop longer crowns when growing in mixtures with pine and pine trees developing larger crown radius in mixtures.

2. Material and methods

2.1 Study area and study design

The study was conducted in boreal coniferous forests in Hedmark county, eastern Norway. Seven stands, with four sample plot each, in mixed stands dominated by Norway spruce and Scots pine were measured during the summer of 2017. Four stands in Løten and three stands in Rena (Figure 1) were established as a part of the research project REFORM, which studies growth of recently thinned mixed stands. However, the basis of my study are laser scans from six stands and 24 of the 28 sample plots. All scanned stands contained a mixture of spruce and pine and all had been thinned about 10 years ago, most likely during winter (Table 1).
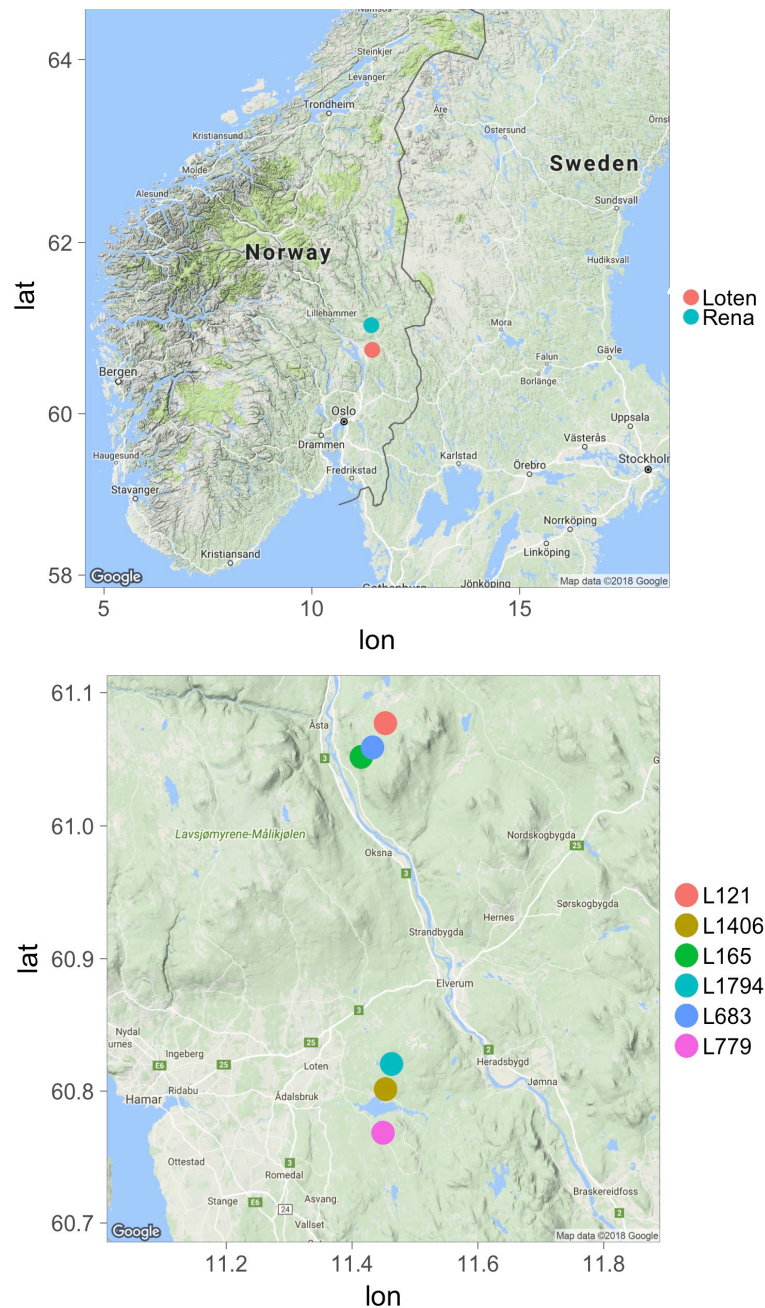

Figure 1. Study locations of the regions (Top) and plots (Bottom) in Hedmark county.

Table 1: Characteristics of sampled stands.

Region	Stand number	Thinned (year)
Løten	779	2006
	1406	2007
	1794	2008
Rena	121	2005
	165	2009
	683	2009

Four circular sample plots were established within each stand, aiming to contain species compositions of (1) pure pine, (2) dominated by pine, (3) dominated by spruce, and (4) pure spruce. This design aimed at capturing the variation in species proportion within each stand in addition to study the mixture effect on individual tree level. The criteria for selection of the sample plots within each stand are described in Attachment 1 (Brunner, 2018). The plots covered a vast part of the species proportion range, which ranged between 11 and 93 percent of the total basal area for spruce and between 6 and 89 percent for pine (Figure 2).
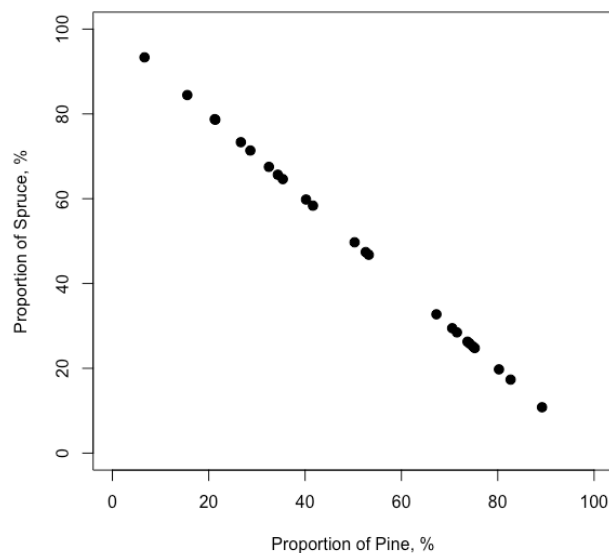
Figure 2. Species proportion in percent of the total basal area for all plots.

The size of the circular sample plots was 531 m^2 with a 13-meter radius from the plot center. However, the laser scanning was mainly focused on scanning trees within a circle of 254 m^2 with a 9-meter radius from the plot center (core plot). The area outside the core plot provided data to describe the competitors to trees close to the edge of the core plot. The median age and site index varied little between the different plots within each stand in both pine (Table 2) and spruce (Table 3), except for stand 779. Site indices indicate growing conditions that are above expected averages for these mixed stands in the region. However, the much more precise measurements of site index on these plots compared to forest inventory data might be the reason for this deviation and growing conditions still representative for most of the mixed stands in the region.

Table 2. Site index and median age per plot for each stand in Scots pine.

Stand	Site index (H$_{40}$, m)*			Median breast height age (years)**		
	Plot 1	Plot 2	Plot 3	Plot 1	Plot 2	Plot 3
779	19	16	17	58	69	66
1406	21	20	20	37	42	39
1794	18	17	18	50	49	47
121	18	18	18	55	55	54
165	18	20	19	53.5	52.5	53
683	18	18	18	47	45	46

* Based on Sharma et al. (2011)

** Based on increment cores at breast height with pith

Table 3. Site index and median age per plot for each stand in Norway spruce.

| Stand	Site index (H$_{40}$, m)*			Median breast height age (years)**		
	Plot 2	Plot 3	Plot 4	Plot 2	Plot 3	Plot 4
779	13	15	18	73	66	51
1406	20	18	17	42	42	41
1794	18	19	18	44.5	44.5	49
121	17	17	19	53.5	54	53
165	17	19	21	55	52	54
683	17	18	17	51	49.5	52

* Based on Sharma et al. (2011).

**Based on increment cores at breast height with pith of trees larger than 12 cm.

After thinning, basal area (m^2ha^{-1}) per plot was in general reduced to about 20 to 30 m^2ha^{-1} (Table 4). The calculated thinning quotient (mean diameter at breast height after thinning divided by mean diameter before thinning) differed between plots within same stands (Table 4). In general, the thinning quotient were higher in pure pine plots, compared to mixed and pure spruce plots, indicating that pine-dominated plots have been thinned from below to a greater extent than mixed and spruce dominated plots.

Table 4: Basal area before thinning (m^2ha^{-1}), basal area after thinning (m^2ha^{-1}), basal area in 2017 (m^2ha^{-1}), DBH (cm) before thinning, DBH (cm) after thinning and the thinning quotient (mean DBH after thinning/mean DBH before thinning) of each plot with information derived from field measurements.

Stand	Plot	Basal area before thinning	Basal area after thinning	Basal area 2017	DBH before thinning	DBH after thinning	Thinning quotient
121	1	44.78	21.84	26.93	13.14	18.58	1.41
121	2	31.79	21.52	26.55	14.64	16.64	1.14
121	3	36.09	23.62	28.93	12.26	12.90	1.05
121	4	32.85	23.19	28.36	12.93	13.87	1.07
165	1	34.7	23.62	29	14.08	18.31	1.30
165	2	36.7	25.42	31.38	16.36	19.87	1.22
165	3	27.53	22.72	27.83	14.64	16.81	1.15
165	4	39.18	31.56	38.57	17.28	19.75	1.14
638	1	34.7	23.62	29	16.72	18.03	1.08
638	2	36.7	25.42	31.38	15.87	16.75	1.06
638	3	27.53	22.72	27.83	19.20	20.36	1.06
638	4	39.18	31.56	38.57	15.45	16.33	1.06
1406	1	34.56	25.76	31.71	13.19	17.89	1.36
1406	2	40.92	30.03	37.07	13.48	16.19	1.20
1406	3	31.27	24.74	30.42	13.95	18.14	1.30
1406	4	28.02	20.34	25.11	13.27	15.39	1.16
779	1	44.2	30.89	38.14	12.17	13.75	1.13
779	2	34	23.59	29.1	16.27	18.01	1.11
779	3	44.5	26.34	32.46	14.58	15.91	1.09
779	4	38.11	24.93	30.62	11.61	12.67	1.09
1794	1	32.1	22.9	27.96	11.96	14.49	1.21
1794	2	31.47	23.15	28.47	11.96	13.10	1.10
1794	3	39.01	25.86	31.85	13.10	14.30	1.09
1794	4	36.08	25.2	30.97	11.97	14.28	1.19

To obtain additional information of the stands compositions and tree size both before and after thinning, diameter distributions were made for each plot and each species. The diameter distributions also indicate that pine have been thinned from below to a greater extent than spruce in plots where several pines were present, which shifted the diameter distribution towards higher diameter classes after thinning (Figure 3). However, there are also examples of this applying for spruce as well (Figure 4). There are also some plots with few pine trees both before and after thinning (Figure 4), and some plots who before thinning had been dominated by one of the species, but after thinning were transformed into more evenly-mixed plots (Figure 5).
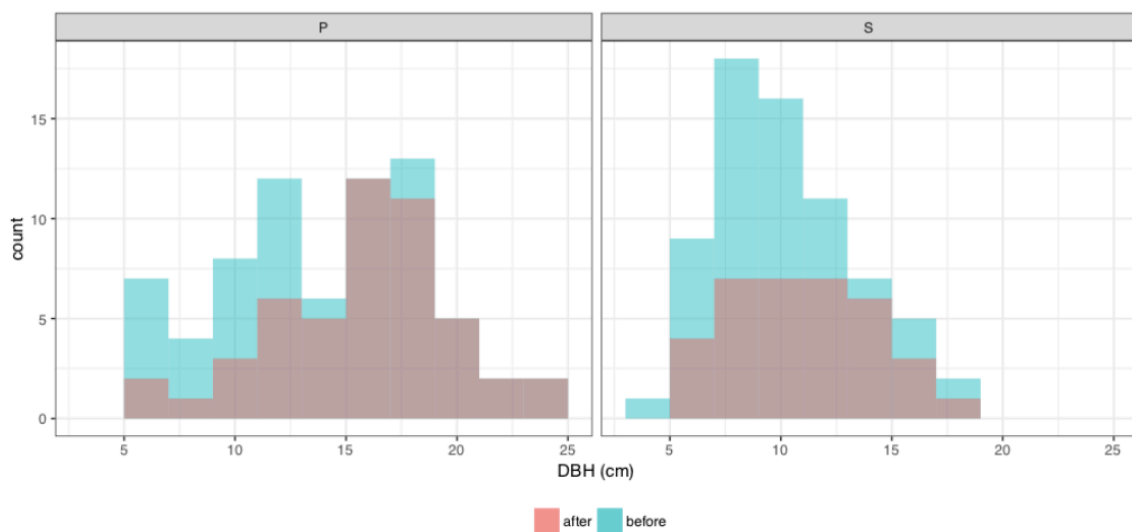
Figure 3. Examples of DBH distributions in pine (P) and spruce (S) from stand 1406, plot 1.
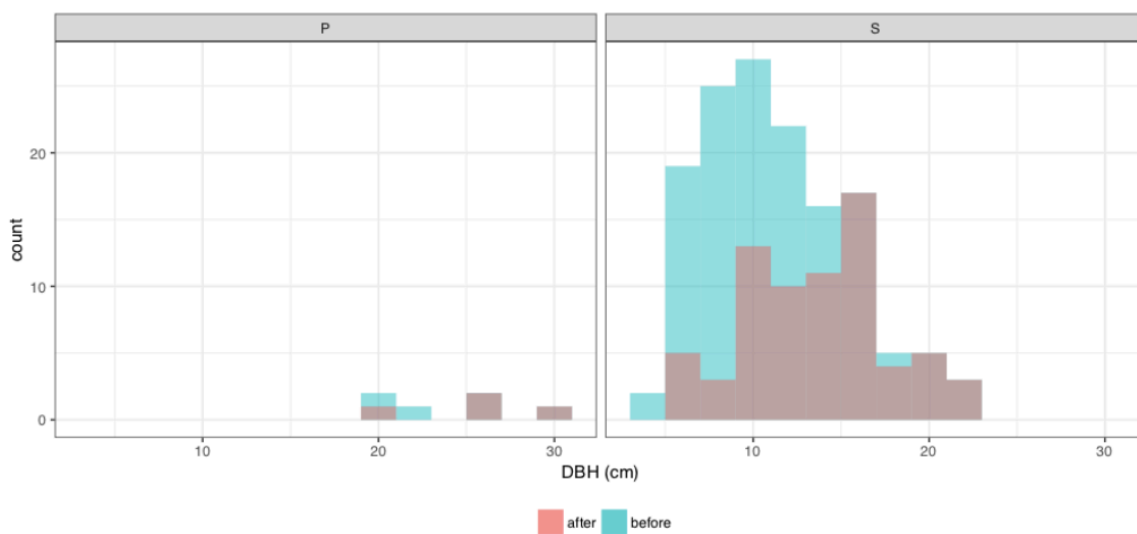
Figure 4. Examples of DBH distributions in pine (P) and spruce (S) from stand 1794, plot 4.

11
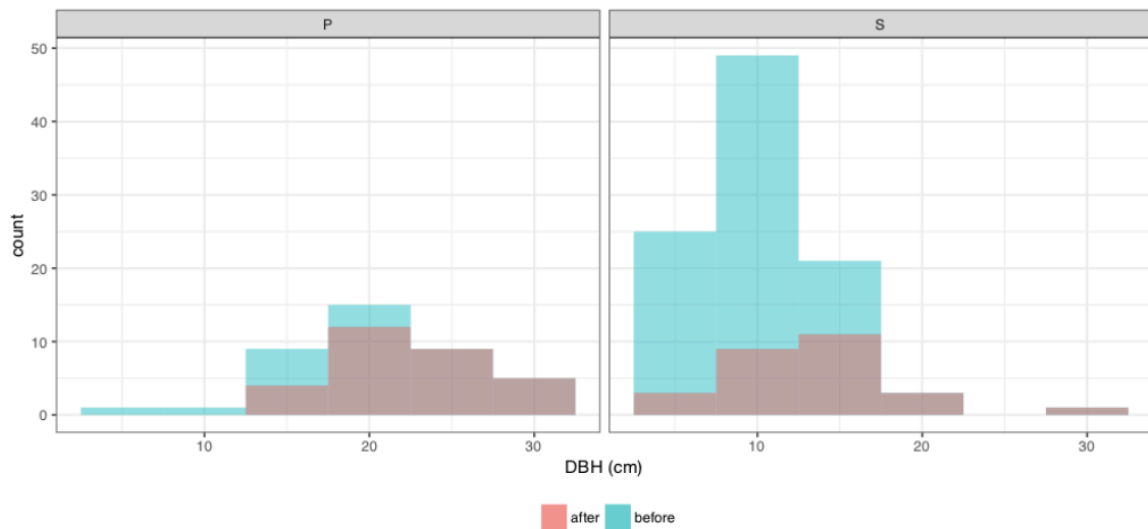
Figure 5. Examples of DBH distributions in pine (P) and spruce (S) from stand 779, plot 1.

2.2 Data collection

2.2.1 Tree measurements

Within each plot, species of the living trees, dead trees, and stumps after last thinning were registered. Using a theodolite and ultrasound distance measurement device, the position and stump diameter were registered for each stump, and tree position and diameter at 1.3 m (DBH) were registered for trees with DBH larger than 5 cm. In addition, height (m) and height to the live-crown base, defined as the height of the lowest living continuous whorl with at least 50 % of the branches being alive and no dead whorl above, were measured for a sample of trees. In pure stands with either spruce or pine, nine trees of the given species were selected as sample trees randomly, evenly distributed across the DBH-range of the given plot. In mixed plots, nine trees of each species were selected for height measurements.

2.2.2 Terrestrial laser scanning

24 plots were scanned with the terrestrial laser scanner Faro Focus[3D] x 130. Since the scanner digitalizes the visible side of the objects, several scans were necessary per plot to provide a complete digitalization of all trees in the core plot. Nine scans were performed in a grid-based design (3 x 3) with approximately 6 meter between each scan. A 10th scan was positioned outside the 3 x 3 grid. The scanning positions were marked in advance with the use of 10 metal poles in gaps where the visibility into tree crowns were sufficient and not blocked by stems and understory trees. In addition, five spheres were set up on wooden poles about 1.5-meter high evenly around the plot center with the purpose of being reference objects when

12

processing the 10 scans into one 3D point cloud. To provide a sufficient co-registration of the scans, we were aiming for a minimum of four visible spheres in each scan. However, five visible spheres were achieved in 210 of the 240 scans. The laser scanner positions were registered by measuring the distance to the four closest living trees or stumps with known positions. The scanner was set on a leveled tripod about 1.5 meter above ground and used with the settings listed in Table 5.

Table 5. Laser scanner settings.

Scanning parameters	Settings
Quality	2x
Resolution	1/4
Scanning resolution (point spacing at 10 m)	6 mm
Horizontal scan range	360°
Vertical scan range	300°
Scan with color	No
Single scan duration	Approximately 2 minutes

2.3 Data processing

2.3.1 Processing point clouds

Faro Scene 6.2 software was used to merge the multiple scans from each plot into one co-registered point cloud per plot. When processing each single scan, the software automatically found the spheres and used them to co-register the entire plot target-based. However, the automatic registration did not always register the targets and therefore some spheres needed to be located manually. Also, automatically found targets who turned out to be false (because of a circular shape of a given diameter) were removed manually in order to increase the accuracy of the co-registration. The target mean distance error from point clouds per plot ranged from 2.4 to 5.3 mm with a mean of 3.1 for all plots. The point cloud per plot was homogenized into 5 mm cells and exported into xyz-files.

2.3.2 Individual tree segmentation

The next step in the data processing was to perform a tree segmentation to obtain crown information from each individual tree by segmenting them according to the method described in Attachment 1 (Brunner, 2018). This was done in the software SAS. In brief, the cells within the sample plots who contained hits from the laser scans were further homogenized into voxels with a size of 0.1 meter. Those voxels were assigned to each individual tree in a four-step procedure, including automatically assigning voxels within a 0.3 meter radius around the stem to the individual trees in addition to using a region-growing algorithm which assigned the voxels that had not been assigned to a tree yet (Attachment 1).

Existing tree segmentation algorithms from TLS are often based on tracing individual branches of deciduous trees in leafless season. In addition, the algorithms are operated on point clouds with scans focused on specific trees in field. In this research, however, the entire core plot was scanned without focusing on individual trees. Scanning coniferous species provided a lower visibility of the highest crown layers, due to foliage further down the stem and/or foliage or stems from neighboring trees blocking the view. Therefore, individual tree segmentation algorithms as used in for example Barbeito et al. (2017), Seidel et al. (2015), and Metz et al. (2013) were not of utility.

When all trees had been processed, the next step was to combine the trees in a plot voxel cloud and correct for further errors, such as voxels being assigned to multiple trees. For some trees, the crown segmentation process and algorithm was not successful, for example because of difficulties in assigning voxels when crowns were overlapping (Attachment 1). Those trees with clear errors needed to be removed before being used in further analysis, resulting in removal of 73 spruce trees and 7 pine trees. For spruce, most of the trees with errors were understory trees with DBH smaller than 12 cm. Those trees had often branches closely to an overstory tree stem and its voxels were assigned to that tree. After removing these trees, 218 pine trees and 398 spruce trees were left in the data and used in further analyzes.

14

*2.3.3 Deriving crown form variable information from crown models*

Crown form information containing individual trees crown radius, crown length and crown volume needed to be derived from each individual segmented tree. In short, a crown model was fitted for each individually segmented tree (Attachment 1). This crown model describes the horizontal distance from the stem center to the branch tips in height layers of 1-meter in a circle divided into 20 directions (Attachment 1). Crown radius was estimated by first calculating the 95-percentile of the horizontal distances of all laser hits in each direction (Figure 6a), then calculating the median distance per height layer (Figure 6b). Applying a moving average for every 3-meter height layer evened out the irregular crown form (Figure 6c) and was used to identify the maximum crown radius and tree height. In addition, the moving average was used to calculate the crown base with the criteria described in Attachment 1 (Brunner, 2018). For pine, the detection of height to the live-crown base (*htcb*) worked out fine and is described in Attachment 1. In spruce trees however, many dead branches were present in lower parts of the stem, affecting the automatic detection of *htcb* and for some trees not even detecting any. For that reason, the height of the maximum crown radius (*ht_maxcr*) was used as a basis to calculate the live-crown length and live-crown volume in spruce and pine trees. This was done assuming the foliage above the height of maximum crown radius is contributing most to biomass production. The crown volume above *ht_maxcr* was calculated by adding the volume from each 1-meter height layer by using a moving average of the median crown radius from *ht_maxcr*. Since the automatic detection of htcb in pine trees were less affected by dead branches, it was used to calculate crown length and crown volume from *ht_maxcr* as well.
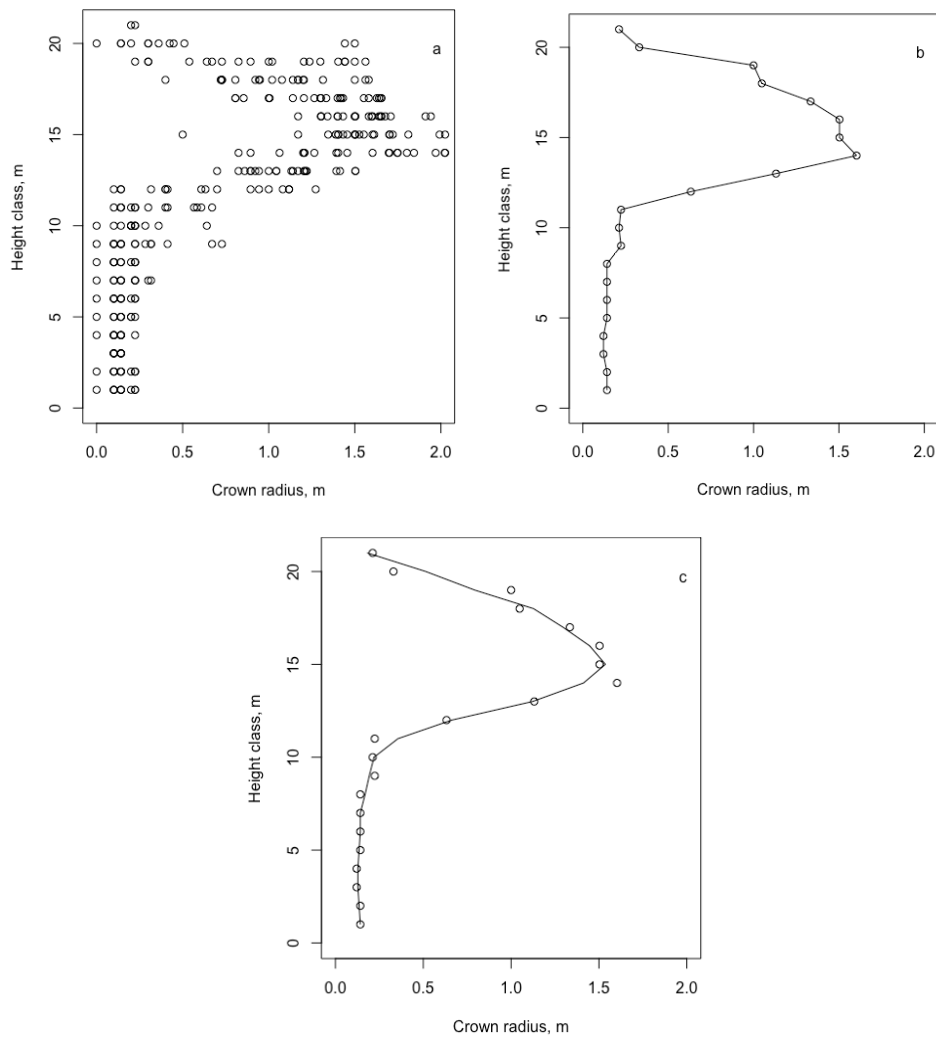
Figure 6. Example of laser data processing from pine tree number 131, plot 3, stand 121, with the calculated 95-percentile of the horizontal distances per 1-meter height layer (a), median distance value per height layer (b), and the moving average for every 3-meter height layer (c).

The number of voxels representing the individual trees differed with the different 1-meter height layers (Figure 7a). Voxels in the lower parts of the trees were often not represented in all 20 directions. This was in general also the case for the top parts of the tree crowns. However, the mid-section of individual trees had often voxel representation in all directions (Figure 7a). This also applied for the number of laser scan hits per 1-meter height layer, with low number of hits in the lower and upper parts of the trees, and a greater amount of laser scan hits in the mid-section (Figure 7b).

16
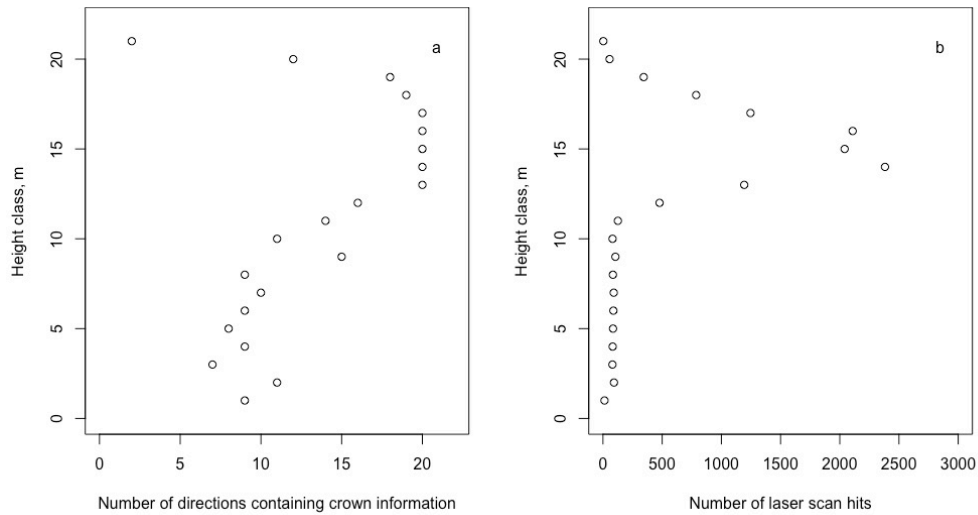
Figure 7. Example of number of directions (max. 20) containing crown information (a) and number of laser scanning hits (b) per 1-meter height layer derived from pine tree number 131, plot 3, stand 121.

2.3.4 Competition index and species proportion

To assess the competition status in 2017 and before thinning, two competition indices were calculated for each of the core plot trees. Competition indices were calculated based on the basal area sum (m^2ha^{-1}) of all neighboring trees within a 4-meter radius around the individual trees in the plot registered as living in 2017 (*Competition index 2017*). Also, the competition status before thinning was described for each tree in the core plot, based on the basal area sum of neighboring trees within a 4-meter radius (*Competition index before thinning*) (Attachment 1). To test for mixture effects on crown form variables, the *proportion of spruce* (in percent of total basal area) was calculated for all trees in the core plots within a 4-meter radius. Some spruce trees did not have neighboring trees within 4-meter radius, but since they grew in almost pure spruce stands, they got assigned 100 % spruce as their species proportion.

2.4 Statistical methods

Further analyses were run in the statistical program RStudio (Version 1.0.153).

Multiple linear regression were used to analyze how species mixtures affects crown length, crown radius, and crown volume. In addition to species proportion, many other variables explain variation in crown variables. Only by including all these effects simultaneously in the model to analyze the unbalanced data, it can be assumed that mixture effects are estimated correctly.

The model for multiple linear regression models has the form:

$$y = \alpha + \beta_1 x_1 + \beta_2 x_2 + ... + \beta_k x_k$$

Where y is the one of the eight crown response variables for spruce and pine described below, and β_i are the parameters for the independent variables x_i listed below.

Maximum crown radius (*CRmax*) (m), crown length from tree height to height of maximum tree crown radius (*CL_CRmax*) (m) and crown volume above height of maximum tree crown radius (*CV_CRmax*) (m^3) were used as response variables in both spruce and pine. In addition, for pine trees, crown length from tree height to height of the live-crown base (*CL_htcb*) (m) and crown volume above live-crown base (*CV_htcb*) (m^3) were used. This means that a total of eight models were made, five for pine and three for spruce.

Six independent variables, who showed high correlation with the crown variables *CRmax*, *CL_CRmax*, *CV_CRmax*, *CL_htcb* and *CV_htcb* were used in the regression analyses. For each response variable, a full model with all the independent variables was tested first and the t-tests were used to indicate the significance of parameter estimates. Variables with insignificant parameter estimates were removed step by step, except for the species proportion variable, starting with variables with the highest p-value. Also, the intercept was not significant for all models. However, they were kept in the models because they did not affect the species proportion effect. The independent variables used in the analysis are:

18

- *DBH* (cm)

- *Tree height* (m)

- *Proportion of spruce* (% of basal area)

- *Competition index 2017* (m^2/ha)

- *Competition index before thinning* (m^2/ha)

- Interaction term between *competition index 2017* and *competition index before thinning*

The data used in this analysis are presented in Table 6. The dataset indicates that pine trees in this study on average have a larger DBH than spruce trees, and that there are no pine trees with a DBH smaller than 9.8 cm or with a height lower than 10.1 meter.

Table 6. Mean and range of the variables used in modelling the different crown variables for trees in the core plot.

|		Pine	Spruce
DBH (cm)	Range	9.8 - 36.2	5.0 - 31.0
	Mean	23.3	16
Height (m)	Range	10.1 - 24.9	4.3 - 24.6
	Mean	19.4	15.8
Proportion of spruce (% basal area)	Range	50.8 - 100	0 - 100
	Mean	34.9	65.2
Crown radius (m)	Range	0.6 - 2.7	0.3-2.4
	Mean	1.5	1.2
Crown length from htcb (m)	Range	3.1 - 1	-
	Mean	9.26	-
Crown length from height of maximum crown radius (m)	Range	2.1 - 10.2	0.7 - 16.5
	Mean	5.8	6.6
Crown volume from htcb (m^3)	Range	6.2 - 135.6	-
	Mean	47.4	-
Crown volume from height of maximum crown radius (m^3)	Range	4.9 - 92.2	0.7 - 127
	Mean	30.4	23.5
Competition index 2017 (m^2/ha)	Range	1.7 - 67.5	0 - 73.6
	Mean	27.4	28.1
Competition index before thinning (m^2/ha)	Range	4.9 - 72.2	0 - 74
	Mean	34.2	33

When modelling crown volume, the independent variables needed to be logarithm transformed due to the non-linear relationship between crown volume and the independent variables. When transforming the two competition indices and the *proportion of spruce* into logarithmic values, 1 was added to the original value, to avoid undefined values in cases of the indices being 0. When presenting model predictions, logarithmic values were back-transformed.

Since the variables *Competition index 2017, Competition index before thinning*, and the interaction between the two indices are all highly correlated, discarding one of these variables may improve the significance level of the others. However, this was not always the case, resulting in all three variables being kept in models where all parameter estimates were significant. By including both competition indices plus the interaction term between them in one model, there might be a multicollinearity problem, causing the variance of the parameter estimates to be inflated. Therefore, the variance inflation factor (VIF) was calculated for each model using R package VIF. VIFs exceeding 10 often suggest a high multicollinearity (O'brien 2007). The models presented in this thesis are not supposed to be used in future predictions of the crown properties. Therefore, multicollinearity that did not affect the species proportion variable were accepted.

3. Results

## 3.1 Crown form variable information

The crown form information from the trees used in this analysis was useful when plotting the crown radius into all directions (max. 20) per height layer above the height of *CRmax*. This was done to evaluate if the rotational symmetric crown model used in the study was a good representation of the crowns, or if crowns extended into canopy gaps in certain directions. For most trees the crowns were symmetric around the stem axis, as illustrated for some typical examples for both pine (Figure 8) and spruce (Figure 9). Typical examples for the vertical crown form illustrates that spruce have longer crowns than pine, and the crown forms are more irregular in spruce compared to pine (Figure 10).
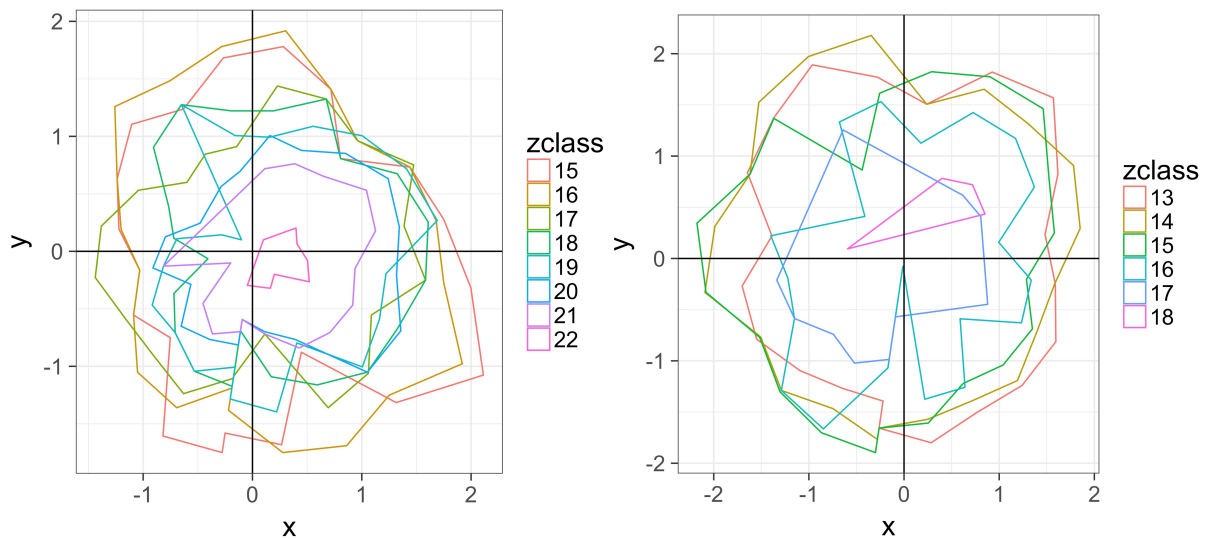
Figure 8. Examples of crown radius in all directions (max. 20) per 1-meter height layer (zclass) above height of maximum crown radius presented for pine trees with tree number 131, plot number 3, stand 121 (Left) and tree number 1, plot 3, stand 1794 (Right).
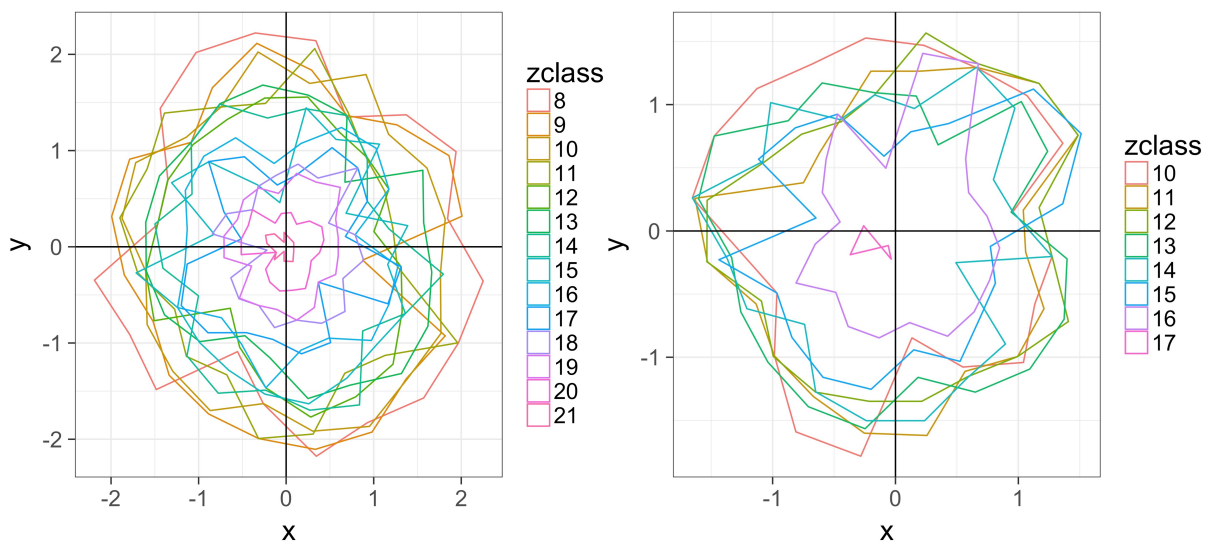

Figure 9. Examples of crown radius in all directions (max. 20) per 1-meter height layer (zclass) above height of maximum crown radius presented for spruce trees with tree number 55, plot 3, stand 165 (Left) and tree number 19, plot 3, stand 779 (Right).
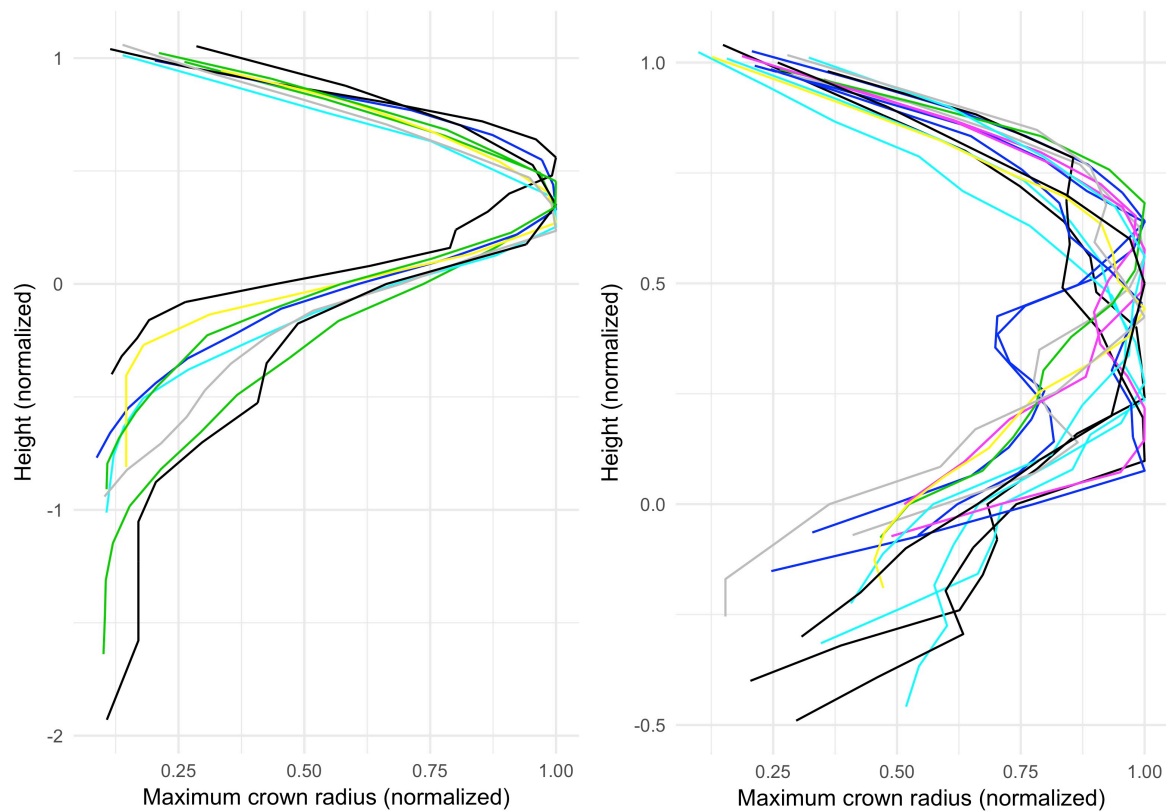
Figure 10. Examples of crown models fitted to laser scanner data for pine (Left) and spruce (Right) normalized to tree height and maximum crown radius, each line represents a tree, in sum representing all trees in stand 683, plot 2.

DBH is the variable which explains most of the variation in the crown variables *CRmax* (Figure 11), *CL_CRmax* (Figure 12), *CV_CRmax* (Figure 13) in both spruce and pine used in this study, in addition for the variables *CL_htcb* and *CV_htcb* in pine (Figure 14). Plotting *CRmax* over *DBH* for the two respective species also reveals that spruce trees in general had longer *CL_CRmax* than spruce (Figure 12b). This also applied for *CV_CRmax* (Figure 13b). Also, the pine trees used in this analysis included less understory trees (>12 cm DBH) and some larger trees (>25 cm DBH) compared to spruce (Figure 15). Some spruces in Rena were larger than spruce in Løten (Figure 15b) resulting in spruces in Løten containing wider *CRmax* (Figure 11b) longer *CL_CRmax* (Figure 12b) and *CV_CRmax* (Figure 13b) compared to spruce in Rena. In pine, on the other hand, there was not much differences within the range of trees in either of the variables between the two regions. Also, pines *CRmax* was slightly larger than spruces (Figure 13).
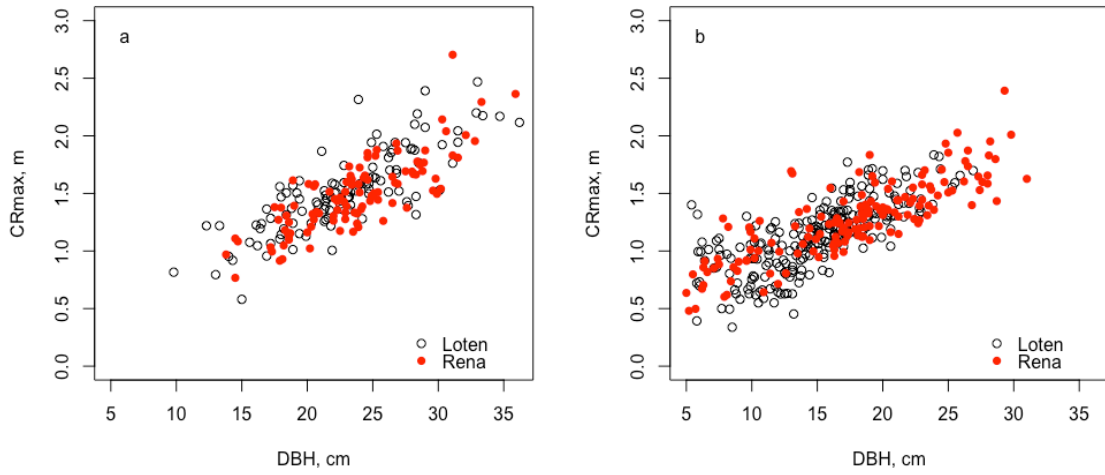
Figure 11. Maximum crown radius over DBH for Scots pine (a) and Norway spruce (b) in regions Løten and Rena.
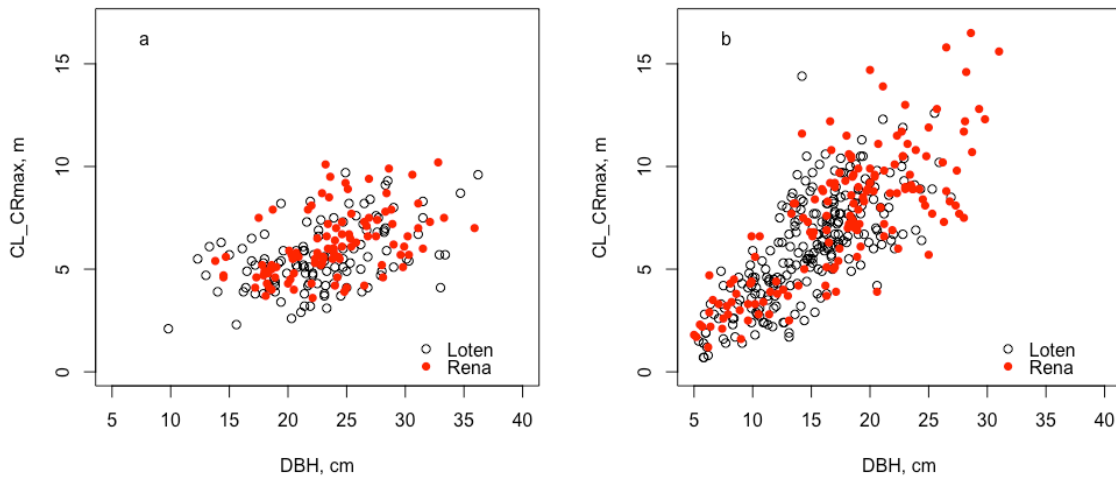
Figure 12. Crown length from height of maximum tree crown radius over DBH for Scots pine (a) and Norway spruce (b) in regions Løten and Rena.
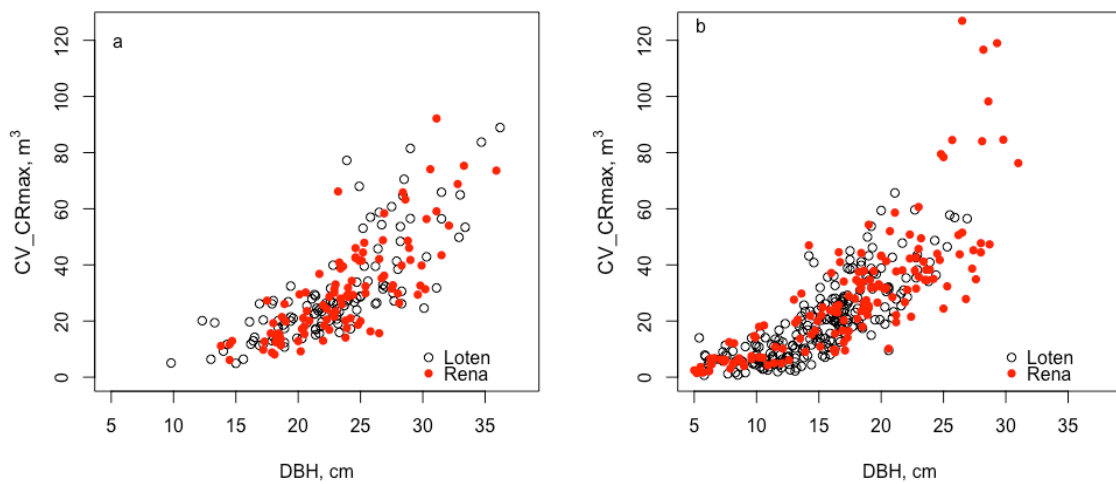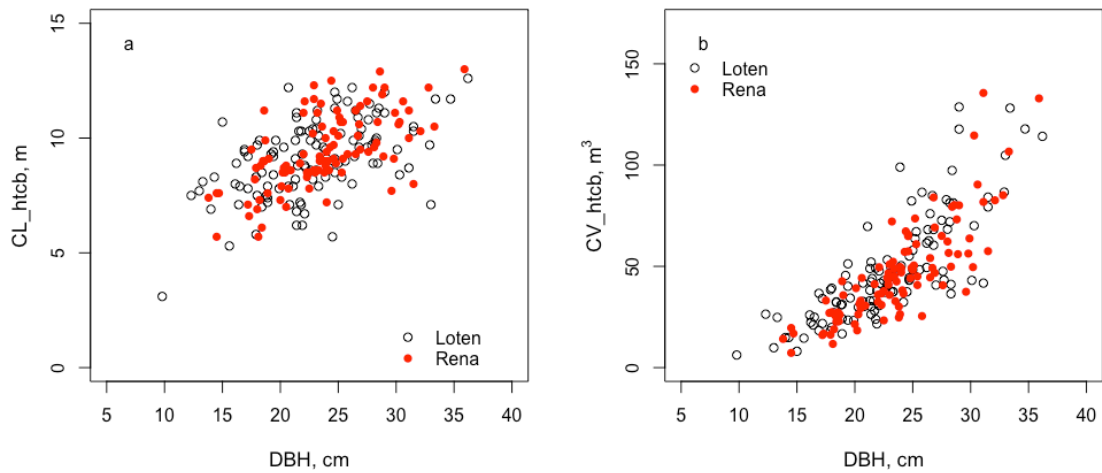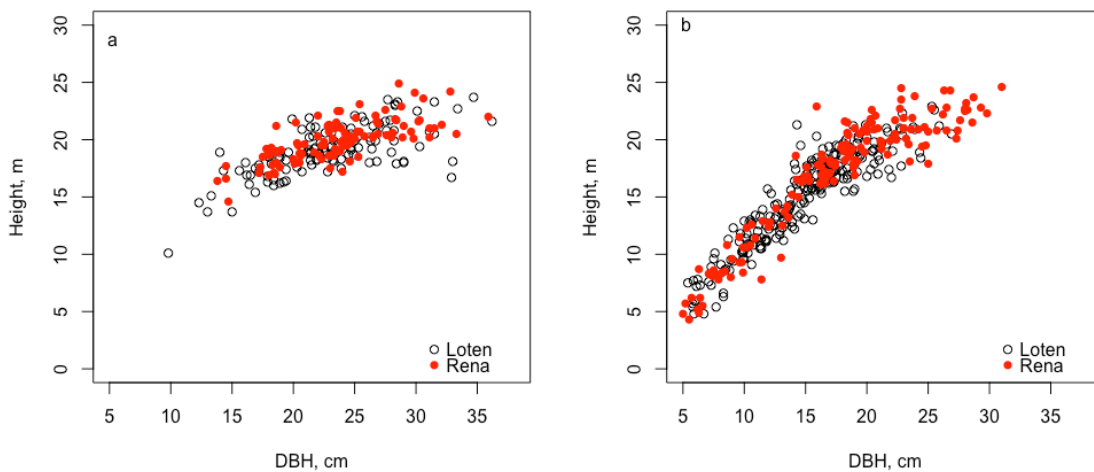

Figure 13. Crown volume above height of maximum tree crown radius over DBH for Scots pine (a) and Norway spruce (b) in regions Løten and Rena.

23

Figure 14. Crown length from height of live-crown base over DBH (a) and crown volume above height of live-crown length over DBH (b) for Scots pine in regions Løten and Rena.

Figure 15. Height over DBH for Scots pine (a) and Norway spruce (b) in regions Løten and Rena.

3.2 Species mixture effect on crown variables in Scots pine

3.2.1 Maximum crown radius

Multiple linear regression analysis testing for species mixture effects on *CRmax* in pine showed a non-significant result with *proportion of spruce* having a p-value>0.05 (Table 7). In addition, none of the VIFs calculated for the variables in this model were larger than 10, indicating that there is no multicollinearity problem in the model. Model residuals plotted against each of the independent variables did not indicate any trends (Figure 16).

24

Pine trees might have crown radius close to or even larger than 4-meter radius. *Proportion of spruce per plot* (i.e. 531 m^{2}ha^{-1}), was used as an additional variable in the model, to test for whether the calculated *proportion of spruce* covered the neighboring trees which directly influenced the pines crown radius. This did not improve the model, and the residuals from the model plotted against *proportion of spruce per plot* did not indicate any trends (Figure 17). Although not presented in this study, a *CRmax* regression analysis with all the six independent, gave an almost significant result for *proportion of spruce* variable with a p-value of 0.06465. All variables in the model were significant, except the interaction term between *Competition index 2017* and *Competition index before thinning*, which had a p-value of 0.06827.

Table 7. Parameter estimates, P-value, variance inflation factor (VIF), root mean square error (RMSE) and R squared for maximum crown radius regression analysis in Scots pine.

	Parameter estimate	P-value	VIF
Intercept	0.9877	2.65e-14 ***	
DBH	0.06699	< 2e-16 ***	2.2523
Height	-0.04566	1.31e-07 ***	2.0658
Competition index 2017	-0.004808	2.69e-05 ***	1.1720
Proportion of spruce	**-0.000569**	**0.167**	**1.0477**
RMSE			0.1787
R-squared (adjusted)			0.7177

*,**,*** indicate significance at the 90%, 95%, and 99% level, respectively.
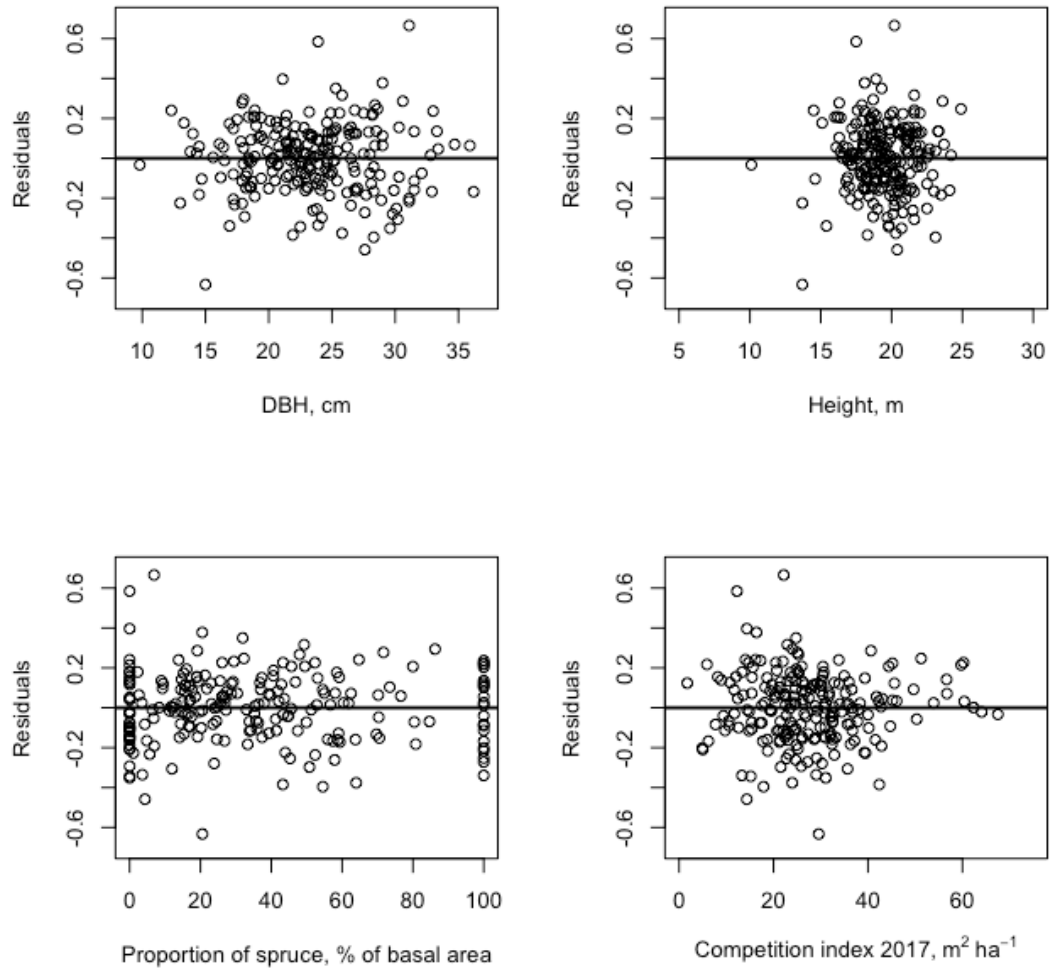
Figure 16. Residuals from crown radius regression in pine plotted against the independent variables.

Figure 17. Residuals from maximum crown radius regression analysis in pine plotted against the proportion of spruce per plot.

3.2.2 Crown length from height of maximum tree crown radius

Species mixture did not have a significant effect on *CL_CRmax* in pine with *proportion of spruce* having a p-value>0.05 (Table 8). However, R^2 was only 0.3191 for this model, indicating a poorer explanation of the variance. None of the VIFs calculated for the variables in this model was larger than 10 (Table 8). The residuals plotted against each of the independent variables did not indicate any trends (Figure 18).
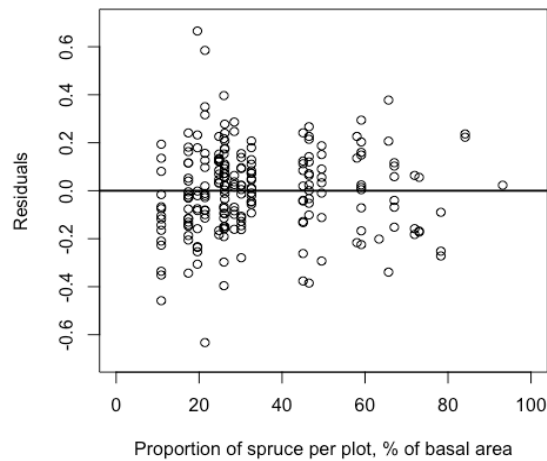
Table 8. Parameter estimates, P-value, variance inflation factor (VIF), root mean square error (RMSE) and R squared for crown length from tree height to height of maximum crown radius regression analysis in Scots pine.

	Parameter estimate	P-value	VIF
Intercept	-1.1551	0.1961	
Height	0.3984	< 2e-16 ***	1.0059
Competition index 2017	-0.02982	0.000199***	1.0398
Proportion of spruce	**0.002**	**0.5135**	**1.0425**
RMSE			1.334
R-squared (adjusted)			0.3191

*,**, *** indicate significance at the 90%, 95%, and 99% level, respectively.

Figure 18. Residuals from crown length from height of maximum tree crown radius regression in pine plotted against the independent variables.
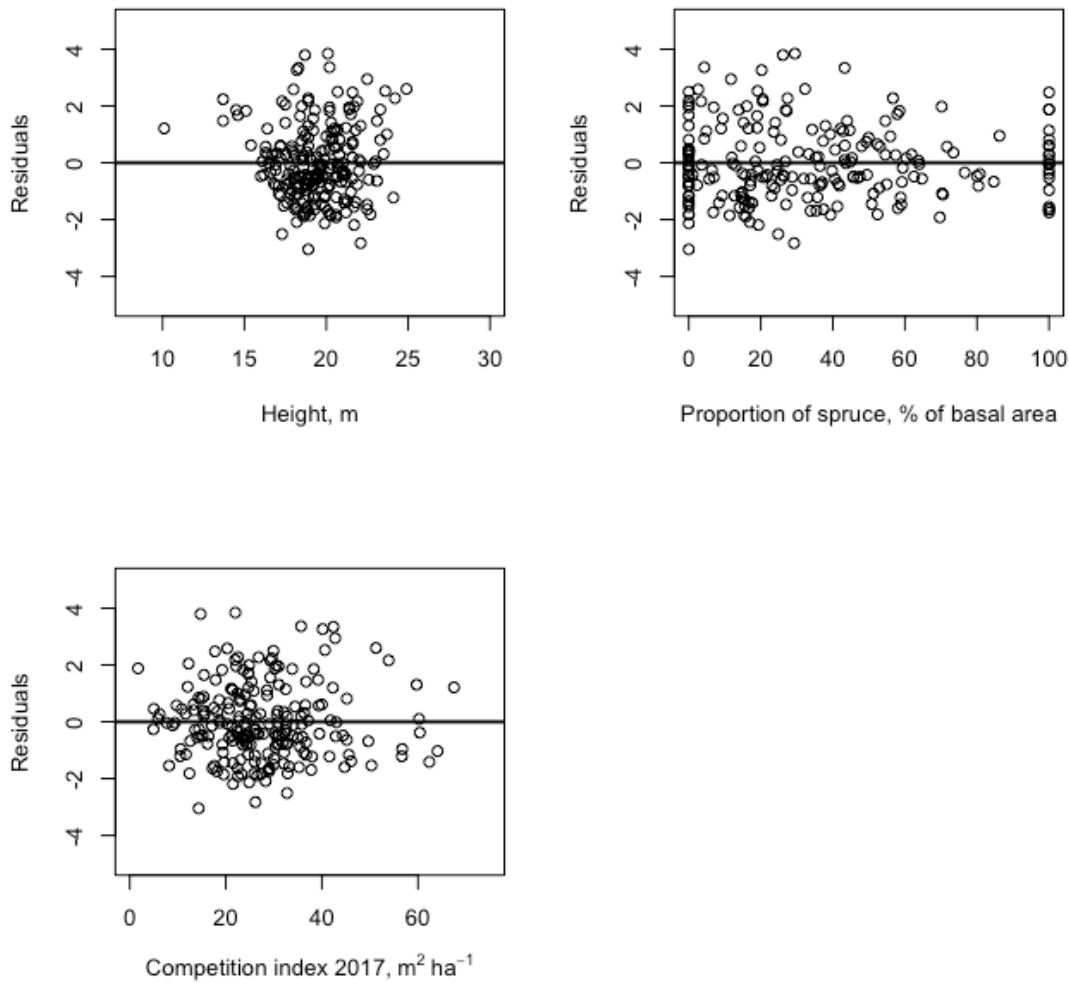
3.2.3 Crown length from height of live-crown base

Species mixture did not have a significant effect on *CL_htcb* in pine with *proportion of spruce* having a p-value>0.05 (Table 9). Also, in this model was the R^2 low, indicating a poorer explanation of the variance. In addition, none of the VIFs calculated for the variables in this model was larger than 10. The model residuals plotted against each of the independent variables in this model did not indicate any trends (Figure 19).

Table 9. Parameter estimates, P-value, variance inflation factor (VIF), root mean square error (RMSE) and R squared for crown length from height of live-crown base regression analysis in Scots pine.

	Parameter estimate	P-value	VIF
Intercept	1.6452	0.0578	
DBH	0.1191	8.23e-06 ***	1.9984
Height	0.2479	4.83e-05 ***	1.9675
Proportion of spruce	**0.0007434**	**0.8025**	**1.0224**
RMSE			1.309
R-squared (adjusted)			0.3674

*, **, *** indicate significance at the 90%, 95%, and 99% level, respectively.

Figure 19. Residuals from crown length from height of live-crown base regression in pine plotted against the independent variables.
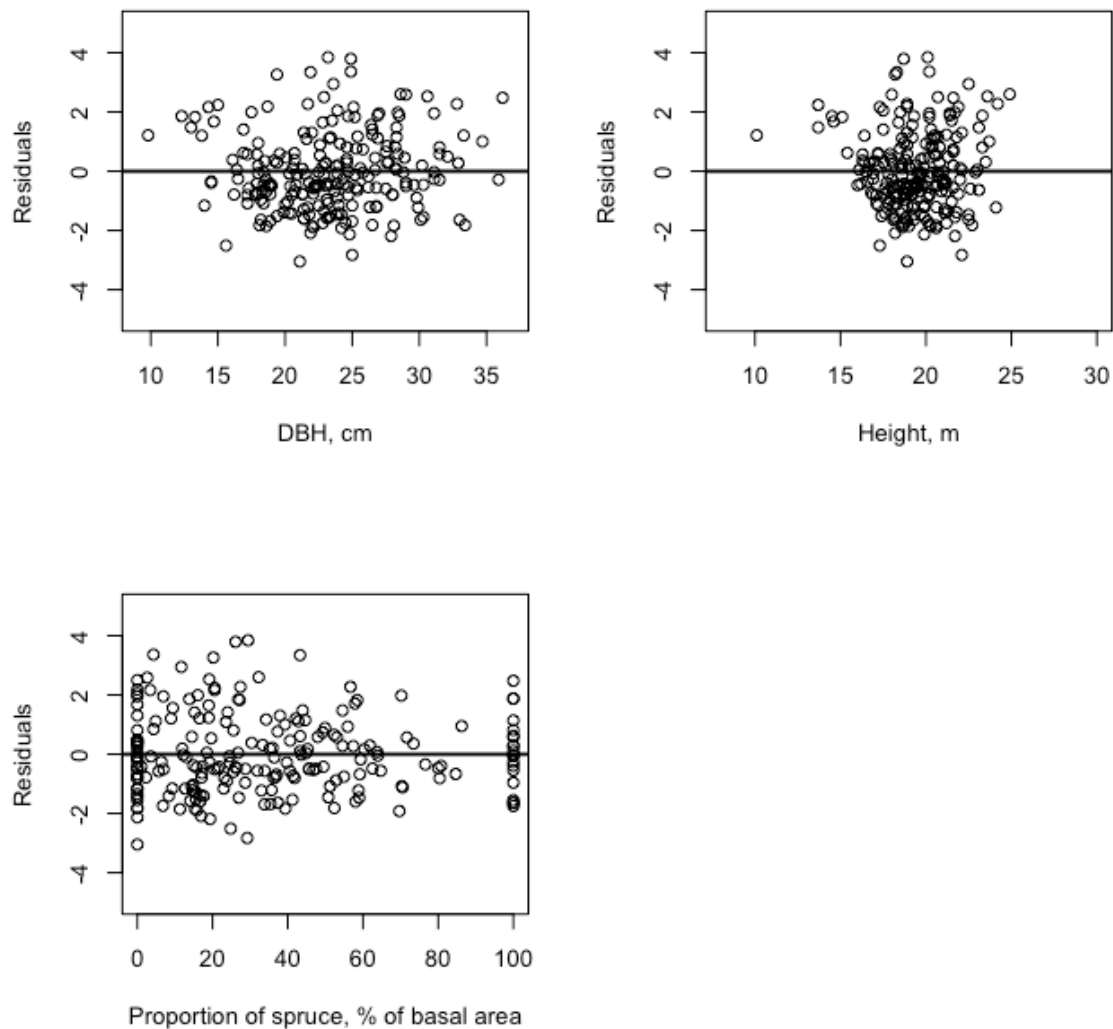
3.2.4 Crown volume above height of maximum tree crown radius

Species mixture did not have a significant effect on *CV_CRmax* in pine with *proportion of spruce* having a p-value>0.05 (Table 10). In addition, none of the VIFs calculated for the variables in this model was larger than 10. The model residuals plotted against the independent variables in this model did not indicate any trends (Figure 20).

Table 10. Parameter estimates, P-value, variance inflation factor (VIF), root mean square error (RMSE) and R squared for crown volume above height of maximum tree crown radius regression analysis in Scots pine.

	Parameter estimate	P-value	VIF
Intercept	-2.1381	5.58e-07 ***	
ln DBH	1.9690	< 2e-16 ***	1.1028
ln Competition index 2017	-0.2339	5.62e-06 ***	1.1032
ln Proportion of spruce	**0.001316**	**0.93**	**1.0062**
RMSE			0.3257
R-squared (adjusted)			0.6747

*, **, *** indicate significance at the 90%. 95%. and 99% level. respectively.
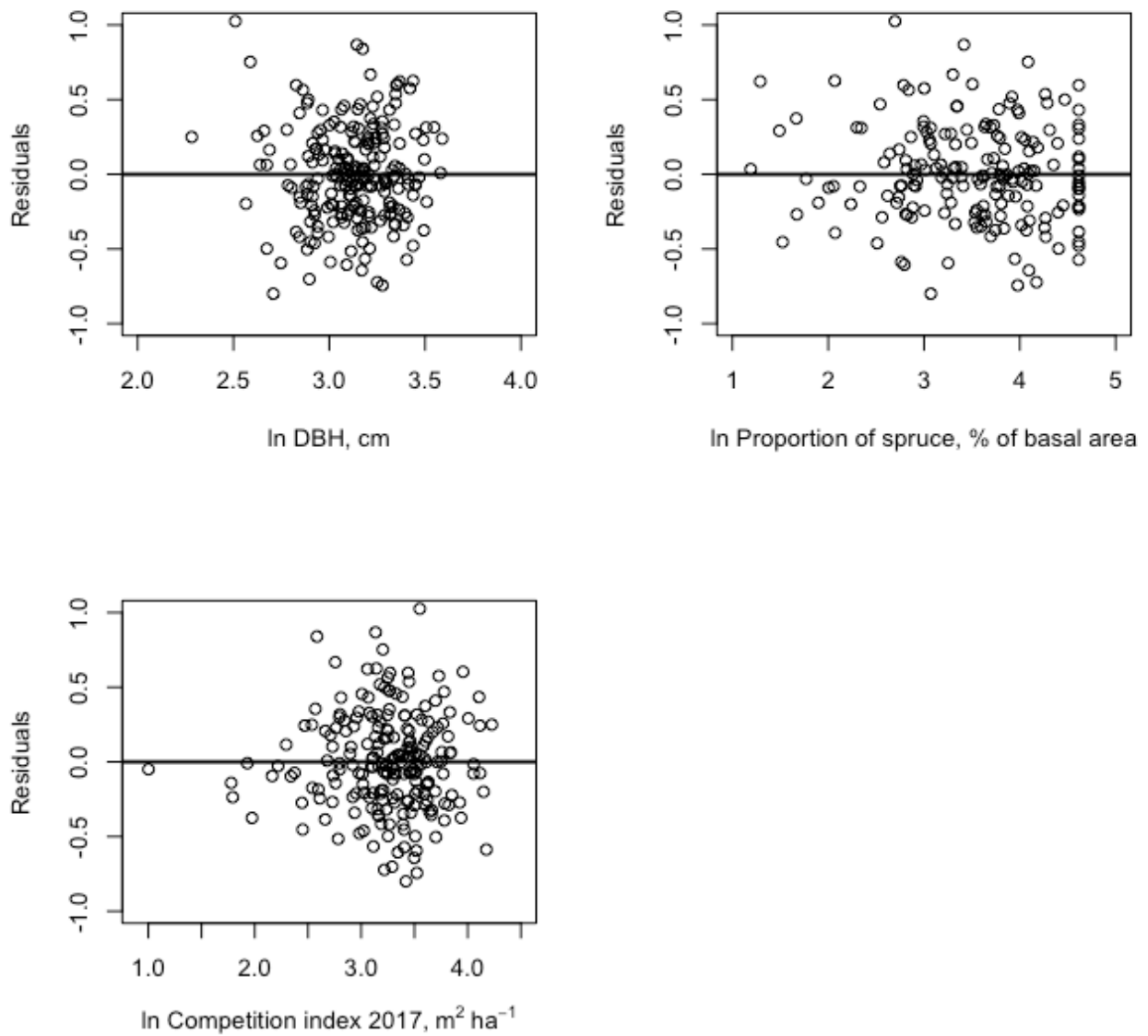
Figure 20. Residuals from crown volume above height of maximum tree crown radius regression in pine plotted against the independent variables.

3.2.5 Crown volume above live-crown base

Species mixture did not have a significant effect on *CV_htcb* in pine with *proportion of spruce* having a p-value>0.05 (Table 11). In addition, none of the VIFs calculated for the variables in this model was larger than 10. The residuals plotted against each of the independent variables did not indicate any trends (Figure 21).

Table 11. Parameter estimates, P-value, variance inflation factor (VIF), root mean square error (RMSE) and R squared for crown volume above live-crown base in Scots pine.

	Parameter estimate	P-value	VIF
Intercept	-1.1659	0.2801	
ln DBH	2.2464	< 2e-16 ***	2.5014
ln Height	-0.5911	0.02248 *	2.3219
ln Competition index 2017 * ln Competition index before thinning	-0.03075	0.00026 ***	1.1497
ln Proportion of spruce	**-0.01016**	**0.4317**	**1.0056**
RMSE			0.2801
R-squared (adjusted)			0.7351

*,**, *** indicate significance at the 90%, 95%, and 99% level, respectively.
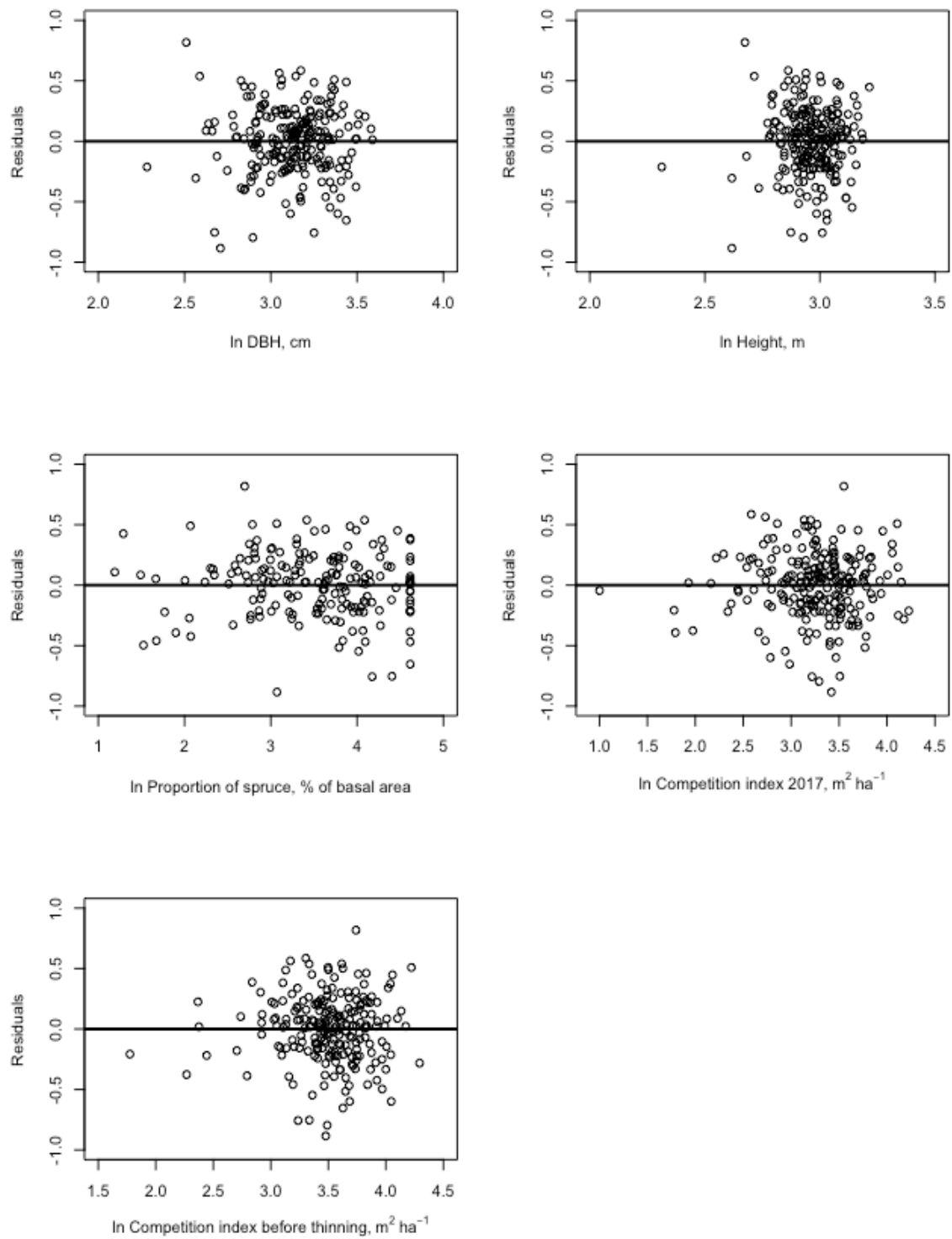
Figure 21. Residuals from crown volume above live-crown base regression in pine plotted against the independent variables.

### 3.3 Mixed-species effect on crown variables in Norway spruce

3.3.1 Maximum crown radius

Multiple linear regression analysis testing for species mixture effect in *CRmax* in spruce showed a significant result with *proportion of spruce* having a p-value<0.001 (Table 12). Increasing *proportion of spruce* by 10% reduces crown radius by 1.4 cm, indicating wider crowns in spruce when *proportion of spruce* decreases. DBH, however, describes most of the crown radius variation. Both competition indices affect crown radius negatively. However, the interaction term between the two competition indices indicates that the *Competition index 2017* affects crown radius differently with different values of *Competition index before thinning* (Figure 22).

Table 12. Parameter estimates, P-value, variance inflation factor (VIF), root mean square error (RMSE) and R squared for maximum crown radius in Norway spruce.

	Parameter estimate	P-value	VIF
Intercept	8.713e-01	< 2e-16 ***	
DBH	4.369e-02	< 2e-16 ***	1.1586
Competition index 2017	-1.121e-02	9.09e-06 ***	8.6146
Competition index before thinning	-4.769e-03	0.02408 *	5.8249
Competition index 2017 * competition index before thinning	1.744e-04	0.00213 **	16.2712
Proportion of spruce	**-1.390e-03**	**1.36e-05 *****	**1.2344**
RMSE			0.1895
R-squared (adjusted)			0.6556

*, **, *** indicate significance at the 90%, 95%, and 99% level, respectively.

Competition indices of 10, 30, and 50 m^2ha^{-1} are common for trees in this study. *Competition index before thinning* was mostly larger than the *Competition index 2017*, with a mean difference of 4.9 $m^2 ha^{-1}$, and a range between -11 and 30 $m^2 ha^{-1}$ (Table 6). Model predictions were therefore made using *Competition index before thinning* of 0, 10, or 20 $m^2 ha^{-1}$ larger than *Competition index 2017* of 10, 30, or 50 m^2ha^{-1} (Figure 22).

Maximum crown radius is predicted to be the widest when trees are growing with less competition around them (10 m^2ha^{-1}) both before and after thinning. With *Competition index 2017* of 10 m^2ha^{-1} and *Competition index before thinning* of 10, or 20 m^2ha^{-1} larger, is the

predicted *CRmax* slightly lower (Figure 22). When *Competition index 2017* was set to 30 m^{2}ha^{-1}, the crown radius were not affected whether *Competition index before thinning* was 0, 30, or 50 m^{2}ha^{-1}. *Competition index 2017* of 50 m^{2}ha^{-1} both before and after thinning, resulted in the smallest crown radius of all in this prediction, although the decrease in *CRmax* was smaller with an increase in *Competition index 2017* from 30 m^{2}ha^{-1} to 50 m^{2}ha^{-1} than a increase in *Competition index 2017* from 10 m^{2}ha^{-1} to 30 m^{2}ha^{-1}. *Competition index before thinning* of 60 m^{2}ha^{-1} or higher only applied for few spruce trees and calculations with those values were therefore not representative or useful in this prediction.
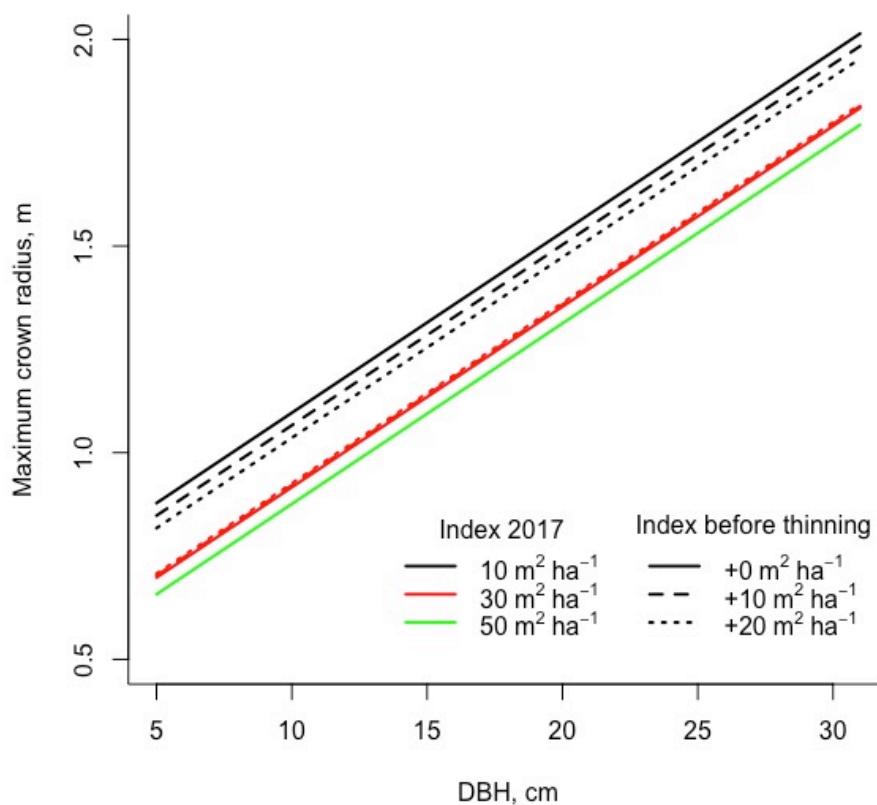
Figure 22. Model prediction for maximum crown radius, with common values of Competition index 2017 (Index 2017) and Competition index before thinning (Index before thinning) 0, 10, or 20 m^{2}ha^{-1} larger than the Competition index 2017 and proportion of spruce set to 50 % (of basal area).

The calculated VIF was 16.27 for the interaction *Competition index 2017 * Competition index before thinning,* indicating a high multicollinearity (Table 12). Despite this, the VIF for *proportion of spruce* variable was 1.2344. Model residuals plotted against each of the independent variables did not indicate any visible trends (Figure 23).
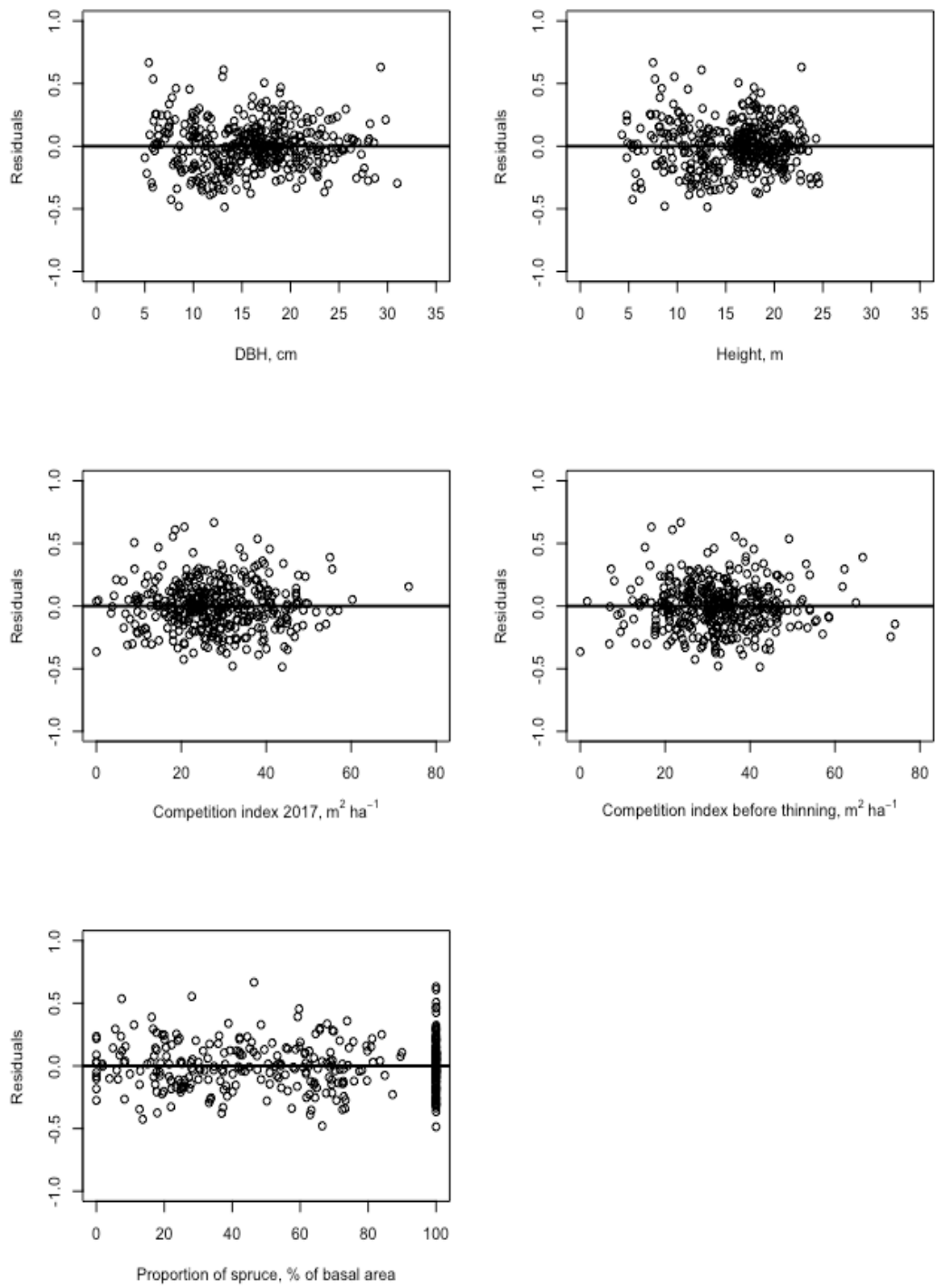
Figure 23. Residuals from maximum crown radius regression in spruce plotted against the independent variables.

3.3.2 Crown length from height of maximum tree crown radius

There is a significant mixture effect in *CL_CRmax* in spruce with *proportion of spruce* having a p-value<0.001 (Table 13). When *proportion of spruce* increases by 10%, decreases crown length by 15 cm. In addition, both competition indices affect crown length negatively, but the interaction term between the two had a positive effect.

Table 13. Parameter estimates, P-value, variance inflation factor (VIF), root mean square error (RMSE) and R squared for maximum crown length from maximum crown length in Norway spruce.

	Parameter estimate	P-value	VIF
Intercept	2.8278	3.40e-05 ***	
Height	0.5110	< 2e-16 ***	1.1067
Competition index 2017	-0.08337	0.000181 ***	8.3527
Competition index before thinning	-0.08710	5.92e-06 ***	5.8551
Competition index 2017 * Competition index before thinning	0.001841	0.000302 ***	16.1714
Proportion of spruce	**-0.01452**	**5.50e-07 *****	**1.2502**
RMSE			1.702
R-squared (adjusted)			0.6732

*, **, *** indicate significance at the 90%, 95%, and 99% level, respectively.

The model prediction for *CL_CRmax* indicates that crowns are the longest when the competition is small, i.e., 10 m^2 ha^{-1} in both *Competition index 2017* and *Competition index before thinning* (Figure 24) However, *Competition index before thinning* of 10 or 20 m^{2}ha^{-1} larger than *Competition index 2017* of 10 m^{2}ha^{-1} results in a decreased *CL_CRmax*. This trend of a decrease in *CL_CRmax* by larger m^{2}ha^{-1} in *Competition index before thinning* also applies when *Competition index 2017* are set to 30 m^{2}ha^{-1}, however the decrease is smaller compared to situations where *Competition index 2017* are 10 m^{2}ha^{-1}. With competition indices of 50 m^{2}ha^{-1} both before and after thinning were the *CL_CRmax* shorter than indices with 30 m^{2}ha^{-1} both before and after thinning, although the reduction is only be some centimeters between the two. As in the previous model prediction, *Competition index before thinning* of 60 or 70 m^{2}ha^{-1} are not representative for the data used in this study.
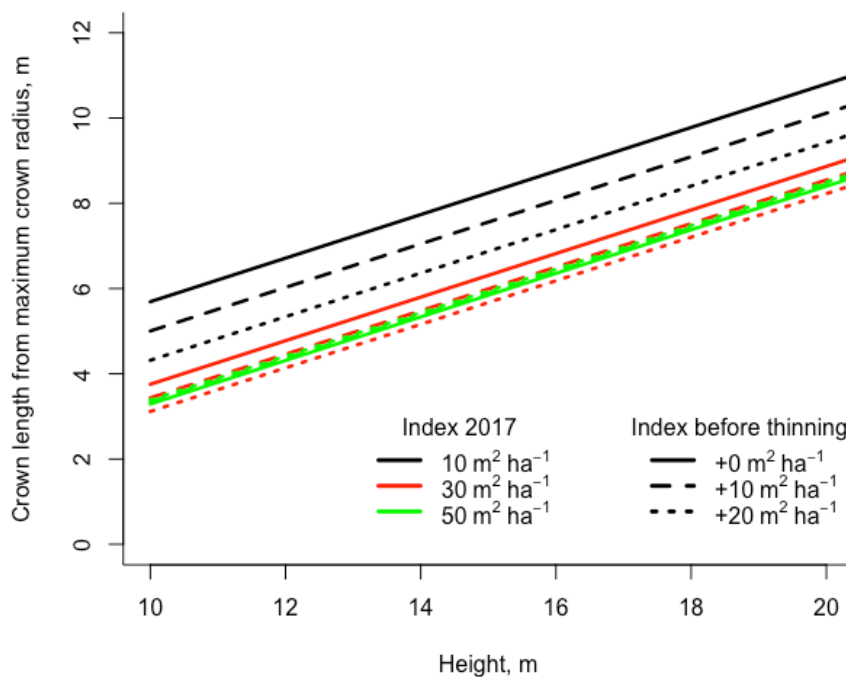
Figure 24. Modell prediction for crown length from height of maximum tree radius with common values of Competition index 2017 (% of basal area) and Competition index before thinning (% of basal area) with a proportion of spruce set to 50 % of basal area.

The residuals plotted against each of the independent variables in this model did not indicate any trends (Figure 25). Both competition indices are significant in addition to the interaction term between the two, with a VIF of 16.17 (Table 19). However, the VIF for *proportion of spruce* is 1.2502.
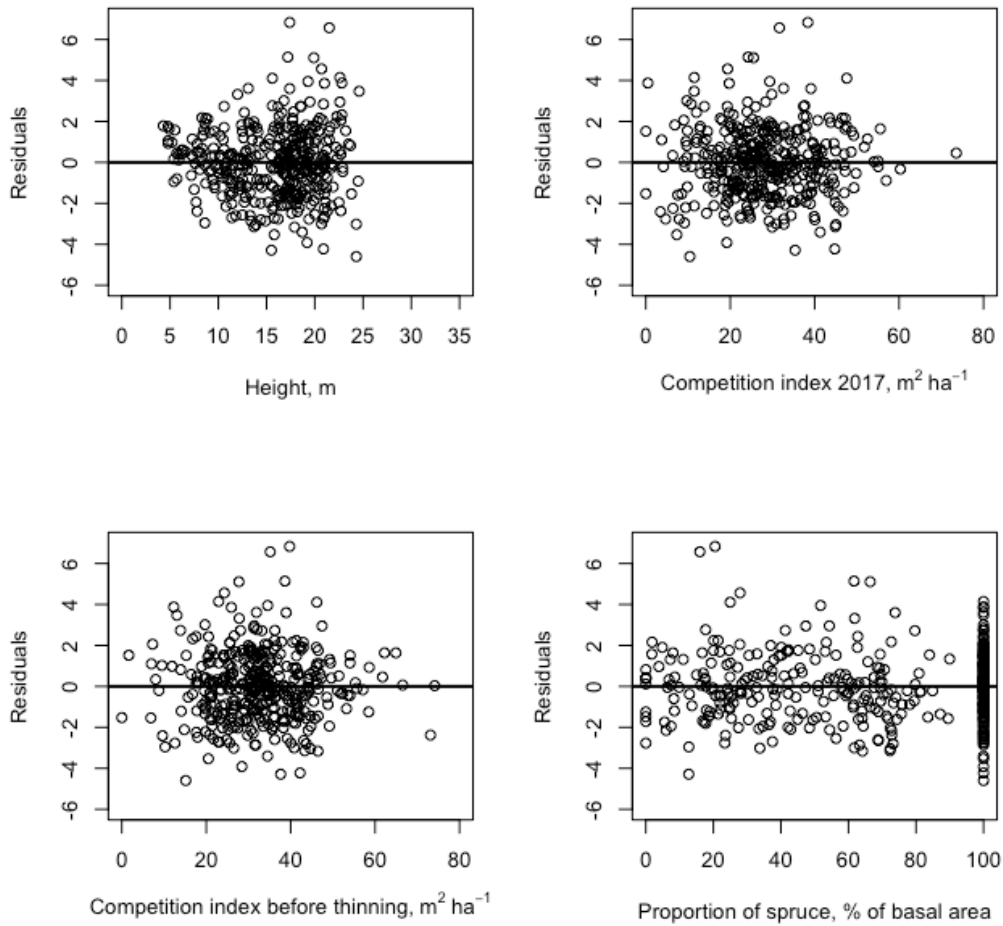
Figure 25. Residuals from crown length from height of maximum tree crown radius regression in Norway spruce plotted against the independent variables.

3.3.3 Crown volume from maximum tree crown radius to tree height

There is a significant mixture effect in *CV_CRmax* in spruce with *proportion of spruce* having a p-value<0.001 (Table 14). VIFs were high for *DBH* and *height* (Table 13), indicating that both variables are highly correlated (Figure 15b). However, they were both kept in the model, because they together increased the R^2 and therefore improved the parameter estimate for the mixture effect. Residuals plotted against each of the independent variables in this model did not indicate any trends (Figure 23).

Table 14. Parameter estimates, P-value, variance inflation factor (VIF), root mean square error (RMSE) and R squared for maximum crown volume in Norway spruce.

Spruce	Parameter estimate	P-value	VIF
Intercept	-1.1049	0.000455 ***	
ln DBH	1.3724	4.09e-11 ***	9.8159
ln Height	0.5679	0.008065 **	9.3688
ln Competition index 2017	-0.2413	6.05e-06 ***	1.2291
ln Proportion of spruce	**-0.1359**	**6.80e-07 *****	**1.0748**
RMSE			0.4866
R-squared (adjusted)			0.7077

*, **, *** indicate significance at the 90%, 95%, and 99% level, respectively
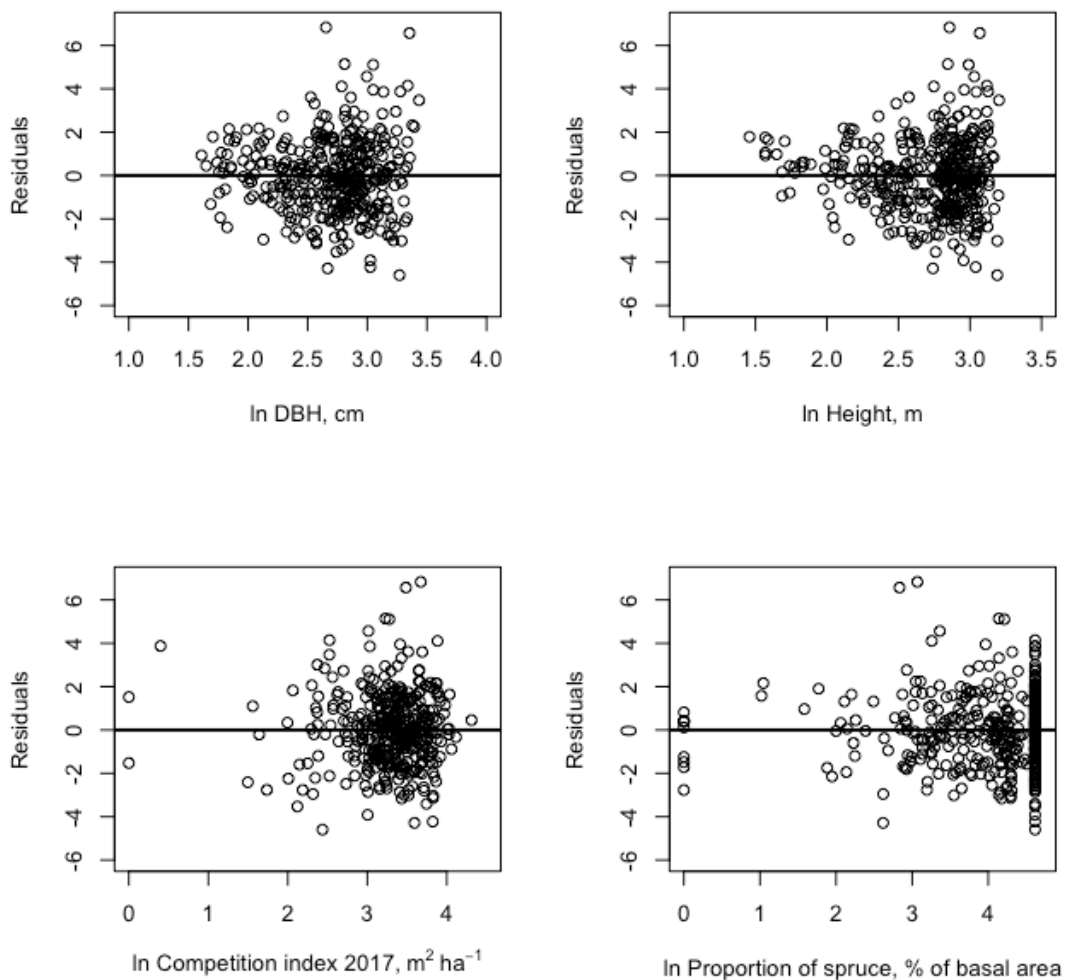
Figure 26. Residuals from crown volume above height of maximal crown radius linear regression analysis in spruce plotted against the independent log transformed variables.

Since all the variables in this model are transformed into natural logarithmic values, model predictions are made to visualize the effect of some of the variables that affect *CV_CRmax* in a non-logarithmic scale. With common values for *Competition index 2017*, model predictions were made for spruce trees in full mixture (i.e. *proportion of spruce* being 50% of basal area). *CV_CRmax* decreases with increasing *Competition index 2017* (Figure 27). The height range of the spruce trees used in this analysis was divided into four height classes which were used in model predictions for spruce trees in full mixtures. *CV_CRmax* increases with increasing height class (Figure 28). With *proportion of spruce* being set to different percentages, model predictions were made. The highest *CV_CRmax* was achieved when spruce is mixed with almost pure pine and decreases with increasing percentage of spruce (Figure 29).
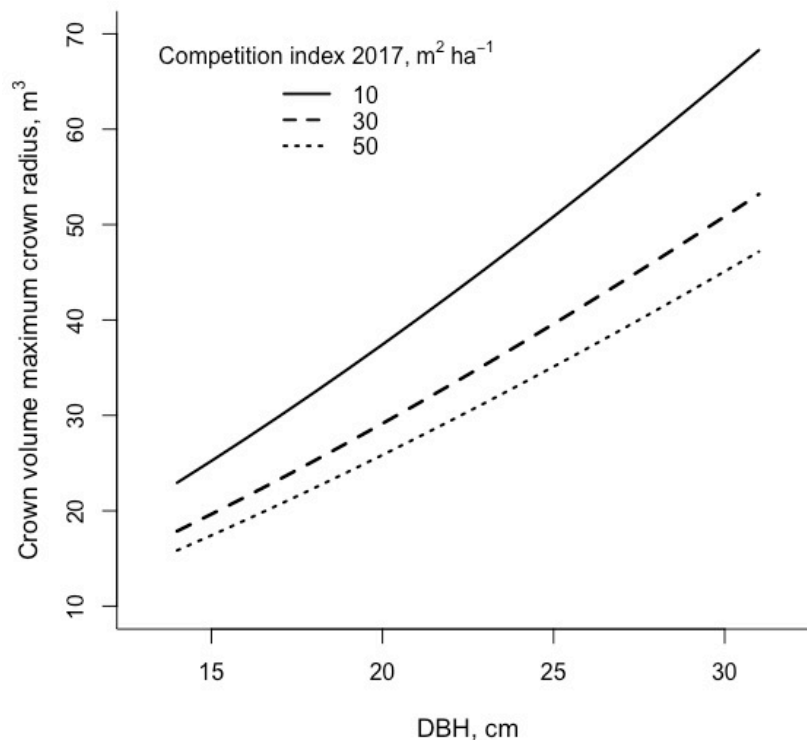
Figure 27. Model prediction with varying Competition index 2017, within the DBH range of height class 21 meter, and proportion of spruce is set to 50 % (of basal area).
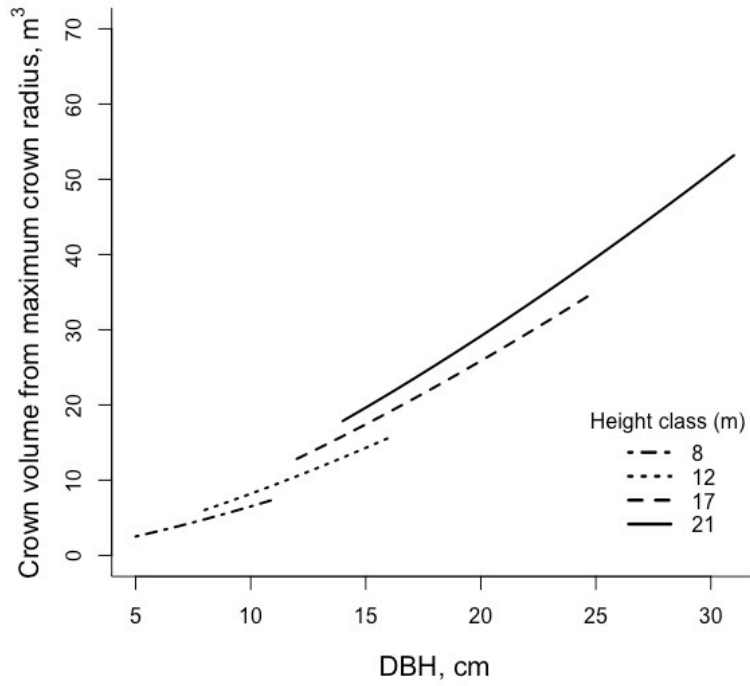
Figure 28. Model prediction with varying height classes, using the DBH range of the respective classes. Competition index 2017 is set to 30 m²ha⁻ and Proportion of spruce is set to 50 % (of basal area).
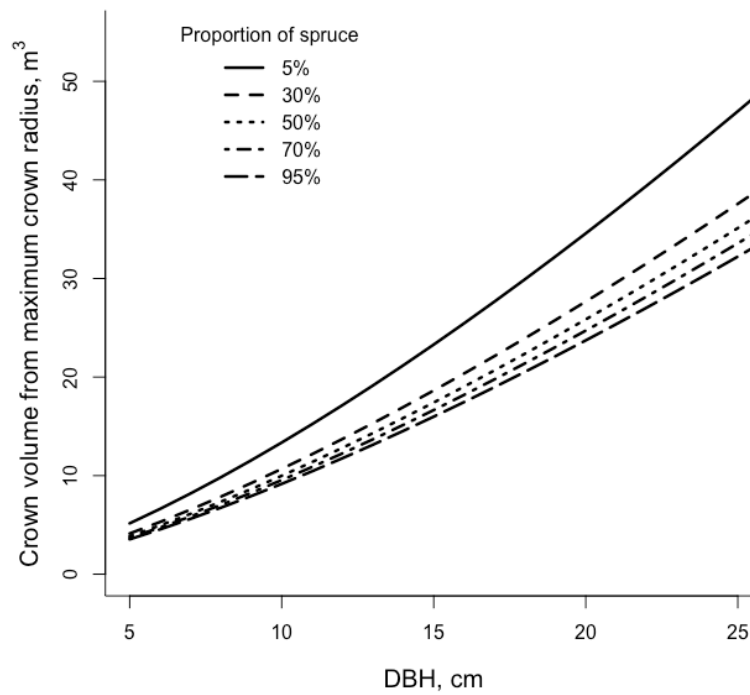
Figure 29. Model prediction with varying proportion of spruce (% of basal area), height set to 17 m and Competition index 2017 set to 30 m²ha⁻¹.

4. Discussion

Tree´s crown form are in general a result of the local environment. If water and nutrient availability are sufficient, light availability is the main limiting growth factor, which trees compete to obtain (Forrester & Albrecht 2014; Perry 1985). Competition and crown form are therefore closely related. The beneficial gain from increased canopy packing in mixtures origins from the idea of mixing species with matching traits might decrease competition between trees. It is therefore beneficial to compare how individual trees reacts to different species proportions within the same growing conditions to quantify any potential mixture effect on crown form. The complementary or non-complementary mixture effect also varies along gradients in resource availability and climate conditions (Forrester & Bauhus 2016), which impact stands site index, stand growth and yield (Pretzsch et al. 2015).

In this study, *CRmax* in spruce was significantly affected by species mixture with crown radius increasing 1.4 cm per 10% decrease in *proportion of spruce* (Table 11)*.* This result coincides with findings in mixtures of Norway spruce and European beech where spruce had significantly longer branches compared to growing in monocultures, despite growing with shade-tolerant beech (Bayer et al. 2013). This implies spruce of having wider crowns when growing in mixtures.

CRmax in pine were not significantly affected by species mixture, although the p-value was 0.167 (Table 6). The parameter estimate from this model, regarding *species proportion* in pine, implies crown width of being 5.69 cm smaller when growing in conditions of 100% *proportion of spruce* as neighbors compared to them growing among pure pine (Table 7). This disagrees with the hypothesis presented in this study, although coincides with findings from mixtures of European beech and Scots pine (Forrester et al. 2018; Pretzsch et al. 2016). These studies revealed a decrease in crown diameter and live-crown length for pine trees growing in mixtures compared to growing in monocultures. This indicates that crown widths in Scots pine abates with the competition in mixtures. European beech on the other hand, increased its crown diameter (Forrester et al. 2018; Pretzsch et al. 2016). However, beech is a more plastic species than both pine and spruce, which suggests that they have a greater ability to grow and maintain large crown forms (Pretzsch 2017). Wellhausen et al. (2017) researched mixtures of Norway spruce and Scots pine, where spruce increased its width by 10% at the expense of pine, which decreased its width by 5% when growing in mixtures, compared to

growing in pure stands. This suggests that there might be too much competition for pine to initiate increased crown width in mixtures with spruce. This statement coincides with findings from research with a different type of pine. Mixtures of Subalpine Fir (*Abies lasiocarpa* (Hook.) Nutt.), Lodgepole Pine (*Pinus contorta* var l*atiofolia* Engelm) and interior spruce ((*Picea glauca* (Moench) Voss.) x (*Picea engelmanni* (Parry) Engelm.)), suggested that pines competitive strength was lower than the spruces when modelling crown radius for the respective species present (Thorpe et al. 2010). However, modelling *CRmax* with all independent variables in this study gave an almost significant result, which may indicate that there is a mixture effect present in pine, although not found in this study.

CL_CRmax in spruce had a significant mixture effect compared to pine where *proportion of spruce* did not have a significant effect on either *CL_CRmax* or *CL_htcb*. This result in spruce coincides with findings in Bayer et al. (2013), who found longer crowns in Norway spruce mixed with European beech. Crown length in pine, on the other hand, had a non-significant effect of mixture in both *CL_CRmax* and *CL_htcb*. This differed from research in mixtures of Scots pine and European beech, where crown lengths in pine decreased in mixed stands with beech present compared to mixed ones (Pretzsch et al. 2015). However, research with mixtures of spruce and pine suggested that spruces crown length increased by 35% in mixtures at the expense of pine, which decreased its length by 5% (Wellhausen et al. 2017). This suggests that there might be too much competition in those types of mixtures for pine to initiate increased crown lengths in mixtures with spruce.

There was a significant mixture effect in *CV_CRmax* in spruce compared to pine where *proportion of spruce* did not have a significant effect on either *CV_CRmax* or *CV_htcb*. In spruce, crown volume increases with decreasing *proportions of spruce*. Larger crown volume in spruce mixed with European beech coincides with research done by Bayer et al. (2013). The volume was calculated by summing the volume from each individual branch with data derived from TLS. The pine models regarding *CV_CRmax* and *CV_htcb*, the R^2 was 0.3191 and 0.3674 respectively. The poor description of the variance in these models might be a result of the small variation in pine trees crown volume compared to volume in spruce trees (Figure 13a and Figure 14b). Also, less understory trees in pine, in addition to only 218 trees used in the analysis, gave less variation in the data compared to spruce.

44

The research who found a decrease in crown width and live-crown length in Scots pine mixed with European beech also found an increase in Scots pines height (Forrester et al. 2018; Pretzsch et al. 2016), which suggests pine trees to shift their crown upwards under competition from other species. If there is to be a mixture effect present in pines crown radius, the crowns need to increase height for them to widen their crown, which might be observable later in the stands development.

The methods used in this thesis also needs to be considered why there were no significant mixture effect in *CRmax* in pine. The *species proportion* were calculated for a 4-meter radius around each tree. Large pine trees may have a crown radius of 4 meter or more, causing the competition indices to not include all competitors of the largest pine trees, resulting in the non-significant result. However, the 13-meter radius plot limited the radius of the *proportion of spruce* calculation. Plotting the residuals from the *CRmax* model in pine over *proportion of spruce per plot* was therefore an alternative in including all the competitors to pine trees (Figure 17), although this might also be an unsuitable method, because it does not include the competition from each individual tree. This variable contains the entire species proportion per plot and does not account for which species are interacting. For example, species might be grouped together in the plot, despite containing an overall 50% species-mixture. Also, the whole plot size might be too large to explain the variance in the core plot trees used in this analysis. Nonetheless, neither plotting the residuals or including the variable *proportion of spruce per plot* in the model suggested that there was a mixture effect in pines crown radius. Including the *proportion of spruce per plot* was also done in the *CRmax* model for spruce, without it improving the model.

The competition between neighboring trees (*Competition index 2017*, *Competition index before thinning* or the interaction between the two variables) was a significant variable in all models, except for *CL_htcb* in pine (Table 8), suggesting that neighborhood competition is an important variable in tree crown development in both species, which are generally in accordance with prior knowledge (Iwasa et al. 1985). The *Competition index 2017* calculated for each tree used in this analysis differed between 0 and 74 m^2ha^{-1}, suggesting that trees grow under quite different competition conditions (Table 6). Model predictions indicated that spruce trees growing under quite low neighborhood competition conditions (e.g., 10 m^2ha^{-1}) both before and after thinning (Figure 22, Figure 24, Figure 27), have grown quite solitary, which is where trees have the ability to maximize their crown form in both crown radius and

crown length (Pretzsch 2017). Reducing *Competition index 2017* to even lower than 10 m^2ha^{-1} will most likely not have any additional positive effect on crown form. Some trees grew under quite high competition conditions, which have suppressed them and prevented them from expanding their crown form. The interaction term between *Competition index before thinning* and *Competition index after thinning* indicates that there is a correlation between the two in how crown form develops with different conditions before and after thinning.

The longest crowns, largest crown radius and highest crown volume for spruce trees growing under full mixture (i.e. *proportion of spruce* is 50%), are predicted to be obtained where *Competition index 2017* is small with 10 m^2ha^{-1} (Figure 22, Figure 24, Figure 27). *Competition index 2017* of 30 m^2ha^{-1} appears to be enough for spruce trees to be suppressed by competition to an amount where they do not increase their *CRmax* regardless if *Competition index before thinning* was 30, 40, or 50 m^2ha^{-1} (Figure 22). When predicting *CL_CRmax* on the other hand, the interaction between *Competition index 2017* and *Competition index before thinning* suggests that there is a difference in *CL_CRmax* when spruce trees are growing under conditions where *Competition index before thinning* was 30, 40, or 50 m^2ha^{-1}, which during thinnings have been decreased to *Competition index 2017* of 30 m^2ha^{-1} (Figure 24). This model prediction insinuates that stronger competition before thinning, results in shorter *CL_CRmax*, however the difference in *CL_CRmax* is much smaller with 40 m^2ha^{-1} in *Competition index before thinning* and *Competition index 2017* of 30 m^2ha^{-1}, compared to if *Competition index before thinning* was 20 m^2ha^{-1} and *Competition index 2017* was 10 m^2ha^{-1}. This indicates that trees growing under less crowded neighborhood conditions prior to the thinning, are more likely to still extend their crown form after thinning because of less competition present and more available light, water and nutrients. If the *Competition index 2017* is still high after thinning, the competition conditions might be too tough for trees to extend their crowns.

Norway spruce is a species which have a greater growth response after thinning (Long et al. 2004). Scots pine on the other hand has a slower response. Since thinning may favor species with the ability to increase its crowns fast, mixed-species forests with those species may close gaps after thinning more quickly (Forrester et al. 2012). This might be the reason for a visible mixture effect in spruce compared to pine. Despite this, the negative mixture effect in pine can also be explained by the initial state of the stands. The stand age indicates that trees in mixed plots have grown between 37 to 66 years together in the stands (Table 2 & Table 3).

However, some plots were more mixed after thinning (Figure 5). If the thinning facilitated the stands into being even more mixed, the crowns have not fully been affected by mixtures during this whole growth period. This could mean that spruce dominating the stands before thinning may have crowded the pines into such narrow crowns that an increase in crown width require pine trees to expand their crown upwards (Jucker et al. 2015). This might occur in future stand development. The pines tree height in this study ranges between 10 and 25 meters, which under further development might increase and under not too crowded neighborhood conditions might induce an increase in crown width. Especially since most of the plots are intermediate to high site conditions (Table 2).

Despite the non-significant mixture effect in pines crown form, it does not mean there are not any present. Pretzsch and Schütze (2016) researched mixture effect on stands who aimed to contain maximum stand density of Norway spruce and Scots pine and found higher stocking densities in mixtures, mainly due to increased amount of stems present in the mixed forests. However, this led to increased crown projection area, which is the sum of the quadratic mean radii of 8 crown radii per tree. The stands used in our analysis are not fully dense, even though the thinning occurred approximately 10 years ago. The basal area in 2017 per plot differed between 25 and 39 m^2ha^{-1} (Table 4), which will increase during the next decade.

Despite the knowledge of coniferous species being less plastic than for broadleaves and having similar growth dynamics, the assumption of pine and spruce both having a mixture effect on crown form, is still present. Pine is a rather vertical oriented, early successional tree species. Spruce on the other hand represent a more horizontally oriented, late successional one. Spruce has a slower growth in which culminates later compared to pine. Pine is also more light transparent than spruce. Spruce as a more shade-tolerant tree, can grow under pines and absorb the light that breaches trough the pines canopy (Forrester 2017). This might increase the total light absorption in a mixture with the two species. In this study however, there were some understory spruce trees, but most of the trees were mono-layered in canopy structure. A more heterogeneous canopy layer might be beneficial in this type of mixture to obtain a greater light absorption, which might be an useful consideration in future silvicultural management aiming to support stands with the two species. For example by planting Scots pine earlier in the rotation. Regardless of the lack of significant mixture effect in pines crown form in this study, and research disagreeing about whether this mixture have a production benefit, this mixture might still be beneficial. For example by increasing habitats for birds

(Gjerde & Sætersdal 1997), increased recreation values or reduced pathogen and risk vulnerability (Felton et al. 2016).

5. Conclusion

The main findings in this study is that there was no significant mixture effect on maximum crown radius, crown length from either height of maximum crown radius or from height of live-crown base or crown volume above either height of maximum crown radius or height of live-crown base in pine. In spruce, on the other hand, there was a significant mixture effect on maximum crown radius, crown length from height of maximum crown radius and crown volume above maximum crown radius. This confirms the hypothesis of longer crowns in spruce and rejects the hypothesis of wider crowns in pine.

6. References

Barbeito, I., Dassot, M., Bayer, D., Collet, C., Drossler, L., Lof, M., del Rio, M., Ruiz-Peinado, R., Forrester, D. I., Bravo-Oviedo, A., et al. (2017). Terrestrial laser scanning reveals differences in crown structure of Fagus sylvatica in mixed vs. pure European forests. *Forest Ecology and Management*, 405: 381-390.

Bauhus, J., Forrester, D. I. & Pretzsch, H. (2017). From Observations to Evidence About Effects of Mixed-Species Stands. In *Mixed-Species Forests*, pp. 27-71: Springer.

Bayer, D., Seifert, S. & Pretzsch, H. (2013). Structural crown properties of Norway spruce (Picea abies L. Karst.) and European beech (Fagus sylvatica L.) in mixed versus pure stands revealed by terrestrial laser scanning. *Trees-Structure and Function*, 27 (4): 1035-1047.

Chambel, M. R., Climent, J., Alía, R. & Valladares, F. (2005). Phenotypic plasticity: a useful framework for understanding adaptation in forest species. *Forest Systems*, 14 (3): 334-344.

De Kort, H., Vander Mijnsbrugge, K., Vandepitte, K., Mergeay, J., Ovaskainen, O. & Honnay, O. (2016). Evolution, plasticity and evolving plasticity of phenology in the tree species Alnus glutinosa. *Journal of evolutionary biology*, 29 (2): 253-264.

Deleuze, C., Hervé, J.-C., Colin, F. & Ribeyrolles, L. (1996). Modelling crown shape of Picea abies: spacing effects. *Canadian Journal of Forest Research*, 26 (11): 1957-1966.

Felton, A., Nilsson, U., Sonesson, J., Felton, A. M., Roberge, J. M., Ranius, T., Ahlstrom, M., Bergh, J., Bjorkman, C., Boberg, J., et al. (2016). Replacing monocultures with mixed-species stands: Ecosystem service implications of two production forest alternatives in Sweden. *Ambio*, 45: S124-S139.

Ford, E. D. (1985). Branching, crown structure and the control of timber production. In Attributes of trees as crop plants. Edited by M.R.G. Cannell and J.E. Jackson. *Institute of Terrestrial Ecology*: 228–251.

Forrester, D. I., Collopy, J. J., Beadle, C. L. & Baker, T. G. (2012). Interactive effects of simultaneously applied thinning, pruning and fertiliser application treatments on growth, biomass production and crown architecture in a young Eucalyptus nitens plantation. *Forest ecology and management*, 267: 104-116.

Forrester, D. I. (2014). The spatial and temporal dynamics of species interactions in mixed-species forests: from pattern to process. *Forest Ecology and Management*, 312: 282-292.

Forrester, D. I. & Albrecht, A. T. (2014). Light absorption and light-use efficiency in mixtures of Abies alba and Picea abies along a productivity gradient. *Forest ecology and management*, 328: 94-102.

Forrester, D. I. & Bauhus, J. (2016). A review of processes behind diversity—productivity relationships in forests. *Current Forestry Reports*, 2 (1): 45-61.

Forrester, D. I. (2017). Ecological and physiological processes in mixed versus monospecific stands. In *Mixed-Species Forests*, pp. 73-115: Springer.

Forrester, D. I., Ammer, C., Annighöfer, P. J., Barbeito, I., Bielak, K., Bravo-Oviedo, A., Coll, L., del Río, M., Drössler, L. & Heym, M. (2018). Effects of crown architecture

and stand structure on light absorption in mixed and monospecific Fagus sylvatica and Pinus sylvestris forests along a productivity and climate gradient through Europe. *Journal of Ecology*, 106 (2): 746-760.

Gamfeldt, L., Snall, T., Bagchi, R., Jonsson, M., Gustafsson, L., Kjellander, P., Ruiz-Jaen, M. C., Froberg, M., Stendahl, J., Philipson, C. D., et al. (2013). Higher levels of multiple ecosystem services are found in forests with more tree species. *Nature Communications*, 4.

Gjerde, I. & Sætersdal, M. (1997). Effects on avian diversity of introducing spruce Picea spp. plantations in the native pine Pinus sylvestris forests of western Norway. *Biological Conservation*, 79 (2-3): 241-250.

Griess, V. C. & Knoke, T. (2011). Growth performance, windthrow, and insects: meta-analyses of parameters influencing performance of mixed-species stands in boreal and northern temperate biomes. *Canadian Journal of Forest Research-Revue Canadienne De Recherche Forestiere*, 41 (6): 1141-1159.

Hackenberg, J., Morhart, C., Sheppard, J., Spiecker, H. & Disney, M. (2014). Highly accurate tree models derived from terrestrial laser scan data: A method description. *Forests*, 5 (5): 1069-1105.

Iwasa, Y., Cohen, D. & Leon, J. A. (1985). Tree height and crown shape, as results of competitive games. *Journal of Theoretical Biology*, 112 (2): 279-297.

Jucker, T., Bouriaud, O. & Coomes, D. A. (2015). Crown plasticity enables trees to optimize canopy packing in mixed-species forests. *Functional Ecology*, 29 (8): 1078-1086.

Lindén, M. & Agestam, E. (2003). Increment and yield in mixed and monoculture stands of Pinus sylvestris and Picea abies based on an experiment in southern Sweden. *Scandinavian Journal of Forest Research*, 18 (2): 155-162.

Long, J. N., Dean, T. J. & Roberts, S. D. (2004). Linkages between silviculture and ecology: examination of several important conceptual models. *Forest Ecology and Management*, 200 (1-3): 249-261.

Longuetaud, F., Piboule, A., Wernsdorfer, H. & Collet, C. (2013). Crown plasticity reduces inter-tree competition in a mixed broadleaved forest. *European Journal of Forest Research*, 132 (4): 621-634.

Metz, J., Seidel, D., Schall, P., Scheffer, D., Schulze, E. D. & Ammer, C. (2013). Crown modeling by terrestrial laser scanning as an approach to assess the effect of aboveground intra- and interspecific competition on tree growth. *Forest Ecology and Management*, 310: 275-288.

O'brien, R. M. (2007). A caution regarding rules of thumb for variance inflation factors. *Quality & Quantity*, 41 (5): 673-690.

Olivier, M. D., Robert, S. & Fournier, R. A. (2017). A method to quantify canopy changes using multi-temporal terrestrial lidar data: Tree response to surrounding gaps. *Agricultural and Forest Meteorology*, 237: 184-195.

Paquette, A. & Messier, C. (2011). The effect of biodiversity on tree productivity: from temperate to boreal forests. *Global Ecology and Biogeography*, 20 (1): 170-180.

Perry, D. (1985). The competition process in forest stands. *Attributes of trees as crop plants*: 481-506.

Pretzsch, H. & Schutze, G. (2005). Crown allometry and growing space efficiency of Norway spruce (Picea abies L. Karst.) and European beech (Fagus sylvatica L.) in pure and mixed stands. *Plant Biology*, 7 (6): 628-639.

Pretzsch, H. (2014). Canopy space filling and tree crown morphology in mixed-species stands compared with monocultures. *Forest Ecology and Management*, 327: 251-264.

Pretzsch, H., del Rio, M., Ammer, C., Avdagic, A., Barbeito, I., Bielak, K., Brazaitis, G., Coll, L., Dirnberger, G., Drossler, L., et al. (2015). Growth and yield of mixed versus pure stands of Scots pine (Pinus sylvestris L.) and European beech (Fagus sylvatica L.) analysed along a productivity gradient through Europe. *European Journal of Forest Research*, 134 (5): 927-947.

Pretzsch, H., Del Río, M., Schütze, G., Ammer, C., Annighöfer, P., Avdagic, A., Barbeito, I., Bielak, K., Brazaitis, G. & Coll, L. (2016). Mixing of Scots pine (Pinus sylvestris L.) and European beech (Fagus sylvatica L.) enhances structural heterogeneity, and the effect increases with water availability. *Forest Ecology and Management*, 373: 149-166.

Pretzsch, H. & Schütze, G. (2016). Effect of tree species mixing on the size structure, density, and yield of forest stands. *European journal of forest research*, 135 (1): 1-22.

Pretzsch, H. (2017). Individual Tree Structure and Growth in Mixed Compared with Monospecific Stands. In *Mixed-Species Forests*, pp. 271-336: Springer.

Seidel, D., Schall, P., Gille, M. & Ammer, C. (2015). Relationship between tree growth and physical dimensions of Fagus sylvatica crowns assessed from terrestrial laser scanning. *Iforest-Biogeosciences and Forestry*, 8: 735-742.

Sharma, R. P., Brunner, A., Eid, T. & Øyen, B.-H. (2011). Modelling dominant height growth from national forest inventory individual tree data with short time series and large age errors. *Forest Ecology and Management*, 262 (12): 2162-2175.

Sorrensen-Cothern, K. A., Ford, E. D. & Sprugel, D. G. (1993). A model of competition incorporating plasticity through modular foliage and crown development. *Ecological Monographs*, 63 (3): 277-304.

Stenberg, P., Kuuluvainen, T., Kellomäki, S., Grace, J., Jokela, E. & Gholz, H. (1994). Crown Structure, Light Interception and Productivity of Pine Trees and Stands. *Ecological Bulletins*,, no 43: pp. 20–34.

Thorpe, H. C., Astrup, R., Trowbridge, A. & Coates, K. D. (2010). Competition and tree crowns: a neighborhood analysis of three boreal tree species. *Forest Ecology and Management*, 259 (8): 1586-1596.

Wellhausen, K., Heym, M. & Pretzsch, H. (2017). Mischbestände aus Kiefer (Pinus sylvestris L.) und Fichte (Picea abies (KARST.) L.): Ökologie, Ertrag und waldbauliche Behandlung. *Allg Forst-und Jagdztg*, 188 (1/2): 3-34.

Attachement 1

Laser scanning of tree crowns in mixed stands of Norway spruce and Scots pine

A method paper

Andreas Brunner, andreas.brunner@nmbu.no, 2018-03-16

This paper describes a method for extraction of individual tree crown metrics from point clouds generated by terrestrial laser scanning. The method has been developed based on data from a large number of sample plots in mixed species stands for the purpose of studying tree crowns and tree growth in these stands. In addition to the laser point clouds, data from field measurements were available and have been used to process laser point clouds. The method is therefore based on a combination of field data and laser point clouds and both methods need to be described in detail to understand the choices taken in method development and the data used in total.

1. Material

Stands

A total of 6 mixed stands of Norway spruce and Scots pine has been selected for this study (7 in total for tree growth study, but stand 897 in Løten was not used for the crown study). The regions of Løten and Rena municipalities in Norway have been selected for this study due to the interest of forest managers for both mixed stands and thinning. We asked specifically for mixed stands that had been thinned about 10 years earlier, in order to study thinning reactions in mixed stands. Additional criteria for selection of stands were:

- homogenous site conditions, i.e. species composition should not be a consequence of site differences,
- variation in species proportions within the stand, but in total a rather equal proportion of both species,
- no fertilization,
- high and homogeneous thinning intensity,
- homogeneous stand density,
- both species represented among the dominant trees,
- no distinct layering of spruce under pine.

Stand characteristics for all sample plots are given in Table 1.

Table 1. Sample plot characteristics
(Site index is dominant height at breast height age 40, using Sharma et al. 2011).

Site	Stand number	Plot number	Species	N (deg)	E (deg)	Laser scanning date 2017	Thinning month	Thinning year	Years since thinning (incl. 2016)	Breast height age spruce (years)	Breast height age pine (years)	Site index spruce (m)	Site index pine (m)	Dominant height (m)	Basal area (m2/ha)	Spruce basal area proportion (%)
Rena	121	1	P	61,0771	11,4540	29.jul		2009	8	56	55		18	22	27	11
Rena	121	2	P(S)	61,0767	11,4513	29.jul		2009	8	53,5	55	17	18	22	27	20
Rena	121	3	S(P)	61,0766	11,4533	29.jul		2009	8	54	54	17	18	21	28	45
Rena	121	4	S	61,0781	11,4531	29.jul		2009	8	53,5	54	19		23	27	72
Rena	165	1	P	61,0518	11,4171	26.jul		2005	12	53,5	53,5		18	22	28	30
Rena	165	2	P(S)	61,0518	11,4128	19.jul		2005	12	55	52,5	17	20	24	31	28
Rena	165	3	S(P)	61,0519	11,4137	19.jul		2005	12	52	53	19	19	23	27	63
Rena	165	4	S	61,0518	11,4149	19.jul		2005	12	54		21		25	37	81
Rena	683	1	P	61,0583	11,4318	26.jul		2009	8	47	47		18	20	28	17
Rena	683	2	P(S)	61,0592	11,4329	26.jul		2009	8	51	45	17	18	20	27	50
Rena	683	3	S(P)	61,0596	11,4342	26.jul		2009	8	49,5	46	18	18	21	24	67
Rena	683	4	S	61,0587	11,4316	26.jul		2009	8	52		17		21	24	93
Løten	779	1	P	60,7688	11,4499	30.jul	spring	2006	11	59	58		19	24	38	25
Løten	779	2	P(S)	60,7690	11,4481	30.jul	spring	2006	11	73	69	13	16	22	29	26
Løten	779	3	S(P)	60,7680	11,4510	30.jul	spring	2006	11	66	66	15	17	22	32	58
Løten	779	4	S	60,7681	11,4520	30.jul	spring	2006	11	51	50	18		21	30	78
Løten	897	1	P	60,7769	11,4033	no	jan-feb	2006	11	35	41,5		21	21	24	21
Løten	897	2	P(S)	60,7770	11,4040	no	jan-feb	2006	11	38	39	21	22	21	24	43
Løten	897	3	S(P)	60,7760	11,4006	no	jan-feb	2006	11	57,5	54	19	19	24	36	68
Løten	897	4	S	60,7761	11,4016	no	jan-feb	2006	11	62		20		26	39	86
Løten	1406	1	P	60,8024	11,4503	27.jul	jan-feb	2007	10	42	37		21	20	31	26
Løten	1406	2	P(S)	60,8008	11,4527	18.jun	jan-feb	2007	10	42	42	20	20	20	37	33
Løten	1406	3	S(P)	60,8019	11,4582	21.jul	jan-feb	2007	10	42	39	18	20	19	30	59
Løten	1406	4	S	60,8007	11,4510	20.jun	jan-feb	2007	10	41	37,5	17		18	25	66
Løten	1794	1	P	60,8197	11,4611	28.jul	jan-feb	2008	9	50	50		18	21	27	21
Løten	1794	2	P(S)	60,8203	11,4621	28.jul	jan-feb	2008	9	44,5	49	18	17	19	28	46
Løten	1794	3	S(P)	60,8207	11,4630	27.jul	jan-feb	2008	9	44,5	47	19	18	20	32	73
Løten	1794	4	S	60,8213	11,4650	27.jul	jan-feb	2008	9	49	51	18		21	30	84

Thinning

Thinning times are indicated in Table 1. Thinnings were from below (add mean diameter before/after thinning) and done by harvesters operating on strip roads, on average removing about

30% of the basal area, from about 35 m^2/ha to about 25 m^2/ha. Thinnings reduced the basal area proportion of spruce on all plots, often by about 10%.

Plots

In each stand, four sample plots with varying species proportions were established, from almost pure pine plots, over pine-dominated mixed plots, and spruce-dominated mixed plots, to almost pure spruce plots. Species proportions for all plots are indicated in Table 1 and range from 11% to 93% spruce of the total basal area in 2017. The sample plot design was inspired by a similar study in mixed stands (Hynynen, Repola et al. 2011). The sampling design will allow studying species mixture effects in each stand on the plot level and individual tree level. The total number of 24 sample plots in this study allows fitting regression models to the plot-level data.

Given the criteria for selection of stands and sample plots, stands were surveyed to identify patches of the desired species mixture in each stand with a minimum distance from stand edges to avoid edge effects. Even tough stands were often large, microsite variation further restricted the population to be sampled from. Sample plots were therefore located based on the list of criteria described above, without any further attempt to randomize their location. The large size of the plots and their location relative to strip roads often only allowed varying the plot center within a few meters.

Circular sample plots with a radius of 13 m (531 m^2) were established. This design allows characterizing neighborhood competition indices using a 4-m radius around each tree for all trees on the core plot (9-m radius, 254 m^2).

During thinning, all tree are removed in strip roads with an average width of about 4 m. The distance between neighboring strip roads is on average 20 m. As a consequence, about 20% of the stand area is directly affected by strip roads and edge trees to strip roads often react with faster crown expansion and growth than trees between strip roads (Makinen, Isomaki et al. 2006). To represent average strip road proportions in circular sample plots is challenging, due to the rectangular design of strip roads as opposed to the circle shape of sample plots. Positioning the plot center about 5 m from a strip road center comes closest to the optimal design. However, this design could not be followed fully due to other restrictions described above and sample plots were most often located in a way that the width of one strip road was entirely included in one edge of the plot, giving similar area proportions affected by strip roads. We registered trees growing at the edge of the strip road and are therefore able to consider strip road affects separately.

2. Methods

Field work tree measurements

For all trees with a dbh larger than 5 cm and stumps (after the last thinning) on the plot, we registered:

- numbers
- species
- stem center position at breast height, only x- and y-coordinates, using a theodolite and an ultrasound distance measurement device
- dbh
- stump diameter
- tree height
- height to crown base

Tree heights were measured for a random stratified sample of 9 trees per species, evenly distributed over the dbh-range found on the plot, on all three plots where this species was expected to be found in large numbers. Based on the tree height sample, height-diameter-regressions were estimated per stand and species using the Näslund equation (Gizachew, Brunner et al. 2012). Residual standard errors of these regressions ranged from 1.2 to 1.7 m. Regressions were used to estimate heights from dbh for trees not measured for height.

[htcb_analyses.sas]

Height to crown base (*htcb*, height to the lowest living continuous whorl, i.e., a whorl that has at least half of the branches alive and no dead whorl above this whorl) was measured for all height sample trees. *htcb* has earlier been shown to be independent of tree size for the same species in closed stands (Purves, Lichstein et al. 2007). This pattern was also found in our data for most sample plots. However, understory trees, of mostly Norway spruce, had a lower *htcb* than overstory trees of the same species. We therefore calculated a mean *htcb* per plot and species separately for overstory and understory (dbh < 10 cm). For plots with missing means for trees in the given class, stand means of *htcb* were used to estimate missing heights to crown base. Only on 3 plots, a regression of *htcb* over dbh showed significant slope parameters for overstory spruce trees, and therefore we applied these regressions to estimate *htcb* from dbh.

Estimated tree height and *htcb* were only used in the first steps of tree segmentation to identify laser hits belonging to individual trees and therefore requirements for precision in these estimates were low.

Laser scanner

Tree crowns on the plots were scanned with a Faro Focus 3D X 130 laser scanner. The scanner uses phase shift technology to measure distance to objects that the laser beam. We used the following settings when scanning the plots:

- Full view angle (360 deg horizontal and 300 deg vertical)
- No colour pictures
- Resolution: ¼
- Quality: 2x

These settings resulted in a resolution of about 6 mm at 10 m distance and a scanning time of about 2 min. per scan.

Laser scanning

The laser scanning design and method was inspired by (Barbeito, Dassot et al. 2017), but modified to scan a large number of tree crowns on the core sample plot with sufficiently high point density rather than individual trees. Ten positions per plot were scanned in a 3 x 3 grid and an additional 10th scan from a strip road in the plot that allowed good visibility (e.g., the opposite strip road that is not included in the plot). The entire set-up of scan position was marked in the field before the scanning. Scan positions were chosen in gaps in the stand with sufficient distance from tree stems and understory trees, and good visibility into tree crowns in all directions. A scan position close to the plot center was selected first, the other positions in the grid were found at about 6 m distance between grid points and a grid orientation parallel to the strip roads. This grid set-up in combination with the plot design also has the advantage that three of the scan positions in the grid are on the strip road with better visibility into tree crowns compared to other grid points in the closed stand.

Figure 1. Set up of laser scanner (tripod), scanner positions (red-white poles), and target spheres in one of the sample plots.

After setting up metal pegs at scan positions (Figure 1), five spheres were set up on wooden poles in the plot center about 1 m above ground, in a way that all five spheres are visible from all 10 scan positions. The spheres were used as targets to automatically co-register the 10 scans. Visibility of spheres was checked from all 10 scan positions, scan positions were moved to ensure full visibility, and branches and understory trees that obstructed spheres were removed.

The scanner was mounted on a leveled tripod at about 1.5 m height. Special care was taken that the tripod was firmly placed on solid ground surfaces and not just resting loosely on mosses. Visibility of the five spheres was checked once again after the tripod had been leveled and before the scan was started. Operators moved out of the field of view of the scanner by hiding behind tree stems or moving around as the scanner moved. All 10 scan positions were scanned successively by moving the scanner on the tripod to the next position. During scanning, the scan position was marked on the ground with flagged metal pegs for later registration of scan positions.

After scanning the entire plot, scan positions were registered by measuring distances to the four closest numbered stems or stumps with known positions, evenly distributed in all directions. An ultrasound distance measurement device was used for this task.

Laser scanning of tree crowns can only produce point clouds with small errors if the tree crowns are not moving during the about 40 minutes of the scanning needed for one plot. This is a challenging task as even light wind moves crowns of 20 m tall trees at the scale of decimeters to meters. Scans were therefore only started if the conditions were promising to be without any wind for the next 2 minutes. In some cases scans had to be repeated to achieve this. No scanning was possible if rain was falling or had been falling before (intercepted water dripping from tree crowns and reflective properties changed by wet foliage).

Laser scanning dates are summarized in Table 1. The entire procedure described above required about 2 hours of work per plot, given perfect weather conditions and no other delays. Accessing the field plots with the heavy equipment on often roadless rugged terrain far from the vehicles required additional hours.

Point cloud processing

The Faro Scene 6.2 software was used for processing of raw data and registration of individual scans into plot point clouds. Sphere targets were automatically detected by the software in individual scans, but hat to be manually corrected to find missing spheres or remove false detections. The number of visible spheres was five for most scans. Only four spheres were visible for 30 of the 240 scans. Automatic co-registration of the 10 scans into a plot point cloud was target-based. The registration accuracy was described by a target error range of 2.4 – 5.3 mm (median 3 mm) for all 24 plots. Plot point clouds were resampled using a cell size of 5 mm to homogenize point density. Plot point clouds were restricted to the plot using scanner positions and spheres to locate the clipping box. Plot point clouds were exported into xyz-files (about 4 GB per plot).

3. Laser crown data processing

For further analyses of the laser point clouds, we used algorithms developed for this purpose and coded in SAS by A. Brunner. Program file names related to the steps described here are given in brackets with the .sas-extension.

The algorithms transformed tree positions into laser coordinate systems, voxelized the point cloud, detected tree positions and dimensions in the voxel clouds, segmented individual tree voxel clouds, and fitted crown models to the voxel clouds of individual trees.

Coordinate system transformation
 [Transform_coordinates.sas, Transform_tree_coordinates.sas]

Scanner coordinates in the point cloud coordinate system were read out from Faro Scene and used to transform tree positions and other x- and y-coordinates measured in the field to point cloud coordinates. As a first step, the scanner position closest to the plot center was used to transform x- and y-coordinates. In four plots, this scan position had larger deviations between scanner and field coordinate systems than the other 9 positions and therefore scan position 1 was used for alignment. In the second step, angular deviations between the two coordinate systems were corrected for, because the field-measured coordinate system was only roughly oriented towards north. For this correction, the direction of the remaining 9 scanner positions from the matched scanner position in step 1 was calculated for both coordinate systems. A least-square regression model was used to estimate the transformation angle.

[In this step, a method to estimate tree z-coordinates, which have not been measured in the field, from scanner z-coordinates has been applied. This procedure uses the same method as described below for the ground cloud segmentation. However, these tree z-coordinates are later replaced by more precise z-coordinates estimated from stem voxels in the ground cloud. The procedure is therefore not described in detail here.]

Voxel clouds
 [Plot_pointcloud.sas]

Point clouds were reduced to voxels with a size of 0.1 m by rounding the x-, y-, and z-coordinate of each laser hit to the nearest 0.1 m and keeping only one position per voxel and no intensity values. The point cloud was further restricted to the field plot by discarding all voxels with a voxel center x-/y-coordinate beyond 13 m distance from the plot center. After this reduction, the plot voxel clouds contained between 476 000 and 750 000 voxels (median 639 000). Z-coordinates of the voxel cloud were transformed to a local coordinate system by substracting the minimum z-value. The plot voxel cloud was segmented into a ground cloud and a tree cloud by sorting all voxels below scanner height into the ground cloud. We were able to use this simple procedure, because we were interested in tree crowns rather than tree stems and could therefore avoid more complex segmentation algorithms that detect the stem base for each tree. Interpolation of z-coordinates indicating scanner height between scanner positions was accomplished by calculating a weighted z-coordinate using all scanner coordinates, which uses the inverse of the distance in the x-y-plane to individual scanner positions as weights for this scanner's z-coordinate. This procedure produced a smooth border between ground and tree cloud and avoided inclusion of ground points into the tree clouds, except for in one plot, where a steep ridge outside the scanner positions could not be modelled by the

weighing procedure and consequently some ground clouds were included in the tree cloud. The ground cloud was used to detect the z-coordinate of the stem base using the lowest z-value of voxels within a cylinder of 0.3 m radius around the stem center position registered in the field. Voxels that were assigned to more than one tree were not assigned to any tree in this step.

Tree segmentation

[Tree_segmentation_crown_core.sas]

Segmentation of individual trees from the plot tree cloud used a four-step procedure: (1) Known tree position and dimensions were used to extract a cylinder of voxels proportional to the tree size, large enough to include all voxels from that tree; (2) Voxels in the core of the expected tree crown were assigned to the tree based on information on tree position and size registered in the field; (3) Voxels assigned to the tree in the crown core are used as seeds in a region-growing algorithm to detect other voxels of this tree within the cylinder extracted in step 1; (4) Segmented tree clouds were combined into a segmented plot cloud and voxels assigned to more than one tree corrected. The first two steps of this algorithm depend on field registered tree positon and size. However, in the absence of this information, stem position and diameter detected in the plot cloud could easily be used to generate this information.

Existing tree segmentation algorithms mostly rely on tracing individual branches in single-tree point clouds scanned from the ground with high point densities, often for broadleaved tree species scanned in the leaf-off phase (Raumonen, Kaasalainen et al. 2013, Tao, Wu et al. 2015, Trochta, Krucek et al. 2017). In our data, point density is rather low in the upper crown, which is a consequence of (a) scanning conifer species, and (b) scanning all trees on a plot from only 10 scan positions without specific considerations about visibility of individual trees.

Measured and estimated tree height and *htcb* were used to detect voxels from these trees. In addition, crown radius was estimated from dbh and tree height using models by (Pretzsch, Biber et al. 2002) for spruce and pine, respectively. Crown radius estimates from these models were reduced to 80% in order to avoid wrong assignments of voxels from neighboring trees when applying these variables.

The voxel cylinder (step 1) had a size of twice the estimated crown radius around the stem axis for the given tree. It was only extracted from the tree cloud after the core crown had been assigned in step 2, causing seed voxels of more than just the focus tree being present.

The core crown (step 2) was defined separately for overstory trees (height > 15 m) and understory trees to avoid that understory trees capture voxels from overstory trees. For overstory trees, a cylinder with the estimated crown radius around the stem axis above *htcb* was used. In addition, all voxels inside a cylinder representing the stem (radius of 0.3 m around stem axis) were assigned to the given tree. For understory trees, only the stem cylinder below a height 2 m under the tree height was assigned to this tree. The very conservative approach for understory trees was necessary to avoid voxels falsely assigned in the tree tip to cause wrong assignments in the next step, as well as branches overlapping with stem sections of larger trees to cause wrong assignments. Voxels that were assigned to more than one tree were not assigned to any tree in this step.

[Tree_segmentation_region_grow_batch.sas]

The 3D region-growing algorithm (step 3) loops through a list of voxels sorted by criteria specified below and identifies for all voxels, that have not been assigned to a tree yet, the 26 voxels that have

direct contact. The voxel is assigned to the most frequent tree found among the 26 voxels. The region-growing was applied twice to the same tree voxel cylinder, firstly, with the voxel list sorted according to ascending z, y, and x, and, secondly, with the voxel list sorted according to descending z, y, and x. This procedure is in the first round growing regions predominantly bottom up, which causes seeds along the stem and lower crown to grow into branches that are pointing upwards. The second round, growing regions predominantly downwards, allows detecting branch segments that are hanging down from other branch segments of the stem. The computation time needed for this step of the algorithm varied between 2 minutes and 40 minutes per tree, depending on the tree size and number of voxels per tree.

 [Tree_segmentation_combine_tree_clouds.sas]

In step 4, individual tree cylinder voxel clouds were combined into a common plot voxel cloud. After the previous two steps of voxels assignments, voxels that were present in more than one cylinder could have been assigned to more than one tree. These double assignments were corrected in step 4. Wrong assignment of branches of neighboring trees often occurred when close proximity of only one or few voxels occurred. The region growing algorithm extended these initial seed voxels to complete branch sections. Voxels with double assignment were assigned to the closest tree using

$$d' = 1 / (\text{distance to stem center} + 1)$$

as a criterion. This distance function is independent of the tree size and gives a lot more weight to trees that are closer to the voxel than to trees further away from the voxel.

This step of the algorithm efficiently assigned double assigned voxels to the correct tree, as long as there were any fully segmented neighbors in the plot cloud claiming these voxels. At plot edges, falsely assigned branches from neighboring trees will not be corrected for. We therefore applied the tree segmentation algorithm to all trees that had a stem center position within 11 m radius from the plot center, to also assign voxels correctly to the neighbors of edge trees on the core plot (9 m radius).

After segmentation, the voxel clouds of individual trees contained between 1 000 and 30 000 to 40 000 voxels, varying with dbh, and with significantly larger numbers for spruce than for pine.

Removal of trees with failed crown segmentation
The crown segmentation algorithm failed for some trees for a number of different reasons. Most often close proximity of trees was the reason. Even though crown overlap almost never occurs in reality in 3D for tall trees due to wind abrasion, the simplifications in the voxel clouds lead to overlap in some cases and the region-growing assigned voxel to wrong trees. Some details in the algorithm were designed particularly to avoid this (search cylinder, conservative assignment of seed voxels), however, without being able to avoid all cases. Particularly for double stems or trees being very close, the algorithm performed poorly. Also understory trees were in general often only segmented with large error. This is a consequence of the often horizontally oriented branches of shade-tolerant spruce trees extended closely to stems of overstory trees. Few leaning trees or snags also caused problems for the algorithm. Removal of double assigned voxels in the algorithm has caused that some branches or crown parts haven't been assigned to any tree, and that the zone of crown shyness might for some trees be much larger than in reality. We have not yet analyzed whether the unassigned crown voxels might have biased crown variable estimates.
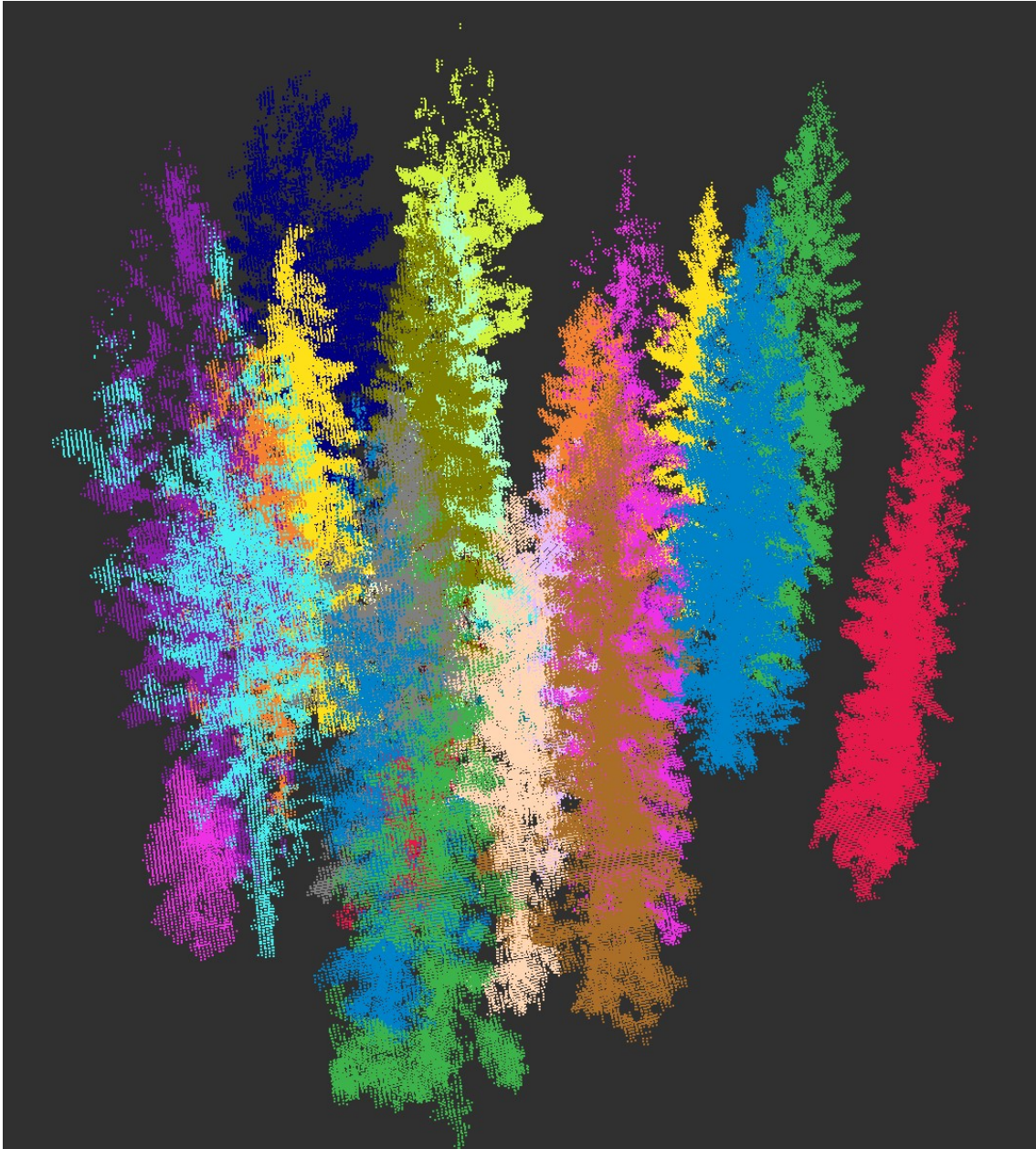
Figure 2. Combined tree voxel cloud after tree segmentation.

We used CompuTree (http://computree.onf.fr) for 3D visualization of voxel clouds, especially when controlling for segmentation errors (Figure 2). All tree in the plot voxel clouds were carefully checked for wrong assignments and trees with failed segmentation identified using stem maps. Other errors were detected using plausibility checks based on crown variables, e.g. a height of the maximum crown radius close to the tree height indicated for many understory trees a failed segmentation. For pine, 7 trees (3%) were removed, leaving 218 trees in the final data set. For spruce, 73 trees (11%) were removed, leaving 389 trees in the final data set. We carefully analyzed the distribution of removed trees in the total data set for variables used to describe crown variables, in order to verify that the final data set was unbiased with regard to all variables. For spruce, most of the removed trees were understory trees with small dbh (Figure 3). No further bias was detected and the focus on

dominant trees in our studies justifies the somewhat smaller representation of these trees in our data.
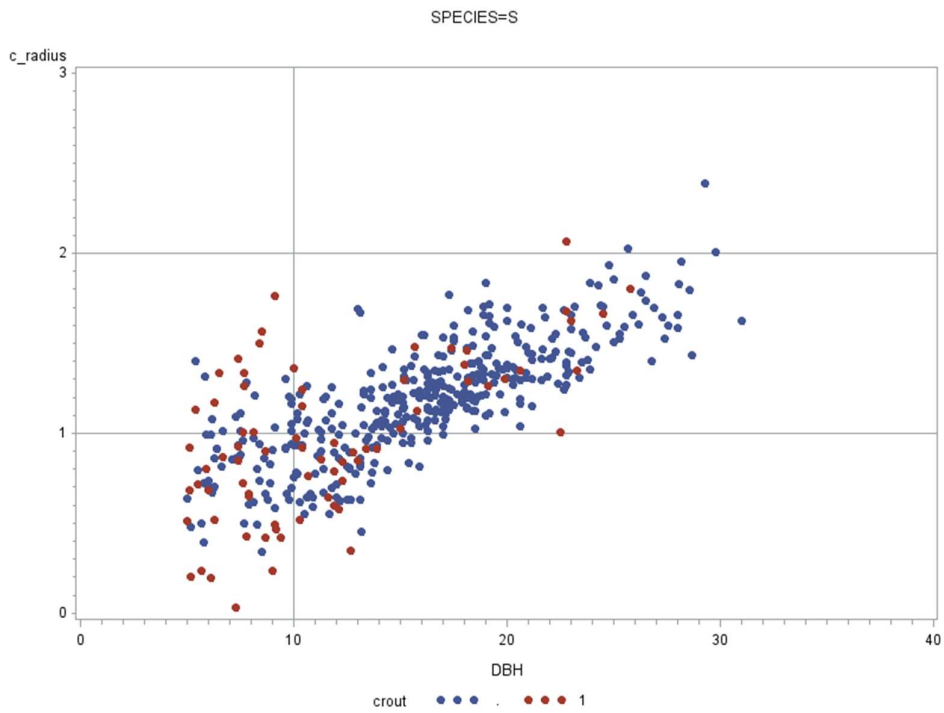

Figure 3. Maximum crown radius estimated from voxel clouds (c_radius, in m) over dbh (in cm) for all spruce trees in the sample. Data marked in red have been removed due to failed crown segmentation.

4. Crown model

[Crown_model.sas]

In order to describe crown shapes and to derive simple crown metrics (crown radius, crown length, crown volume) for further testing, we fitted rotational symmetric crown models to the voxel clouds of every tree.

In a first step, voxels far above the rest of the tree voxel cloud were removed as outliers. Vertical distances of larger than 1 m were considered as indicators for outliers. The maximum z of voxels in the tree cloud above the minimum z ground cloud was used as laser estimated tree height. Laser estimated tree heights were compared with field measured or estimated tree heights for verification. Outlier voxels were only removed for few trees.

Crown models that are rotational symmetric around the stem axis need to define a stem axis which is close to the real stem axis. Field measured stem positions deviated from stem positions in the voxel cloud. We therefore estimated the stem center axis directly from the voxel cloud at this stage. [Earlier the field measured stem positions were used for tree segmentation. However, requirements for precision are much lower in these steps.] For this, a section of the tree voxel cloud of about 3.5 m length was extracted, i.e., from the base of the tree voxel cloud (about 1.5 m above ground) to 5 m above the tree's z-coordinate detected in the ground voxel cloud. In this section, the 12 voxel columns with identical x- and y-coordinates were identified as stem voxels, assuming that with the given voxel size (0.1 m) and stem diameters (max. 0.3 m) a 4 x 4-matrix with in empty core of about 2 x 2 voxels represents the stem. Voxel columns were only accepted if they contained at least 25 voxels. Mean x and y of the accepted voxel columns were used to estimate the stem center position. Voxel columns with a distance of larger than 0.3 m from the mean were removed as outliers and the means recalculated.

Only in a few cases, this algorithm failed due to understory trees growing close to the stem sections and being falsely assigned to these trees. These cases could be detected by comparing field measured stem coordinates with voxel cloud coordinates and identifying distances above 0.2 m as potential errors. After visual inspection of the voxel cloud stem sections, the correct stem center could be found, or in a few cases the field measured position had to be accepted. Differences between tree positions detected from voxel cloud and measured in the field were mostly below 0.2 m and most often below 0.1 m.

For each voxel in the tree cloud, the horizontal distance from the stem axis was calculated and used to describe crown expansion in horizontal directions. The tree voxel cloud was divided into 1-m height classes and within each height class into 20 direction sectors with equal angular extent. For each sector, the 95-percentile of horizontal distances from the stem center was used as an indicator of crown radius in that direction in that height layer. Using the 95-perenctile removes assignment errors from neighboring trees and excludes voxels from branch tips that extend far beyond the general crown shape. Per height layer, the median of all 95-percentiles of crown radius was used to indicate the crown radius of that height layer in the rotational crown model. The median, once more, removes assignment errors from neighboring trees and excludes extreme branch tips.

Plotting median crown radius per height layer versus height (Figure below) shows a typical crown shape. However, variation in crown radius between layers is often large, especially in the upper crown where only few voxels and sectors represent the crown, but also at the crown base due to individual whorls with few branches causing irregular shapes. We therefore applied a moving average with a window of 3 height layers to fit a more regular crown model. For the largest height

layer, a crown radius of 0 m in the layer above was added to calculate the average. In the lowest height layer, which always occurred along the stem at about 1.5 m height far below the tree crown, the lowest radial median was repeated once more for a height layer below.

Maximum crown radius and its height was detected by finding the height layer with the maximum moving average of median crown radii.

Crown base was detected from the moving average of median crown radii by applying two alternative rules that indicate crown recession as moving down the stem axis in successive height layers. Both rules apply crown recession in percent of the maximum crown radius. The first rule assigns an indicator of 1 if crown radius recession exceeds 10%, or an indicator of 2 if it exceeds 20%. Indicators are summed as moving down from the height of maximum crown radius. If the sum of indicators exceeds 1 this height layers is identified as crown base, i.e. if a recession of 20% per meter or two times 10% per meter is needed to detect the crown base. The second rule sums absolute crown recession for all height layers below maximum crown radius and identifies the crown base when this sum exceeds 40%. Both rules very often resulted in the same *htcb*, but more often rule 2 resulted in a lower *htcb* than rule 1 (see Figure below).

Automatic detection of *htcb* resulted in reasonable results that agreed well with field-measured *htcb* for all pine trees (Figure 4, Figure 5). Pine trees in the data were characterized by few large branches below the crown base. The median radius of the voxel cloud therefore receded quickly to values indicating the stem radius below the crown base.

Spruce trees in our data are characterized by a high density of dead branches, often all the way to the ground (Figure 5). The high amount of fine side branches in recently died branches makes it also difficult to distinguish between dead and live branches in that species. For these spruce trees, rule 1 failed as crown radius was reduced successively in small steps, never exceeding 10% of maximum crown radius. We therefore used *htcb* detected with rule 1 in most cases, and only *htcb* detected with rule 2 in cases where rule 1 failed. Detection of *htcb* from the voxel cloud produced realistic results for all 218 pine trees in the final data set. However, only for 335 of the 389 spruce trees, any *htcb* was detected, and even among those 335 trees, *htcb* was often unlikely to indicate the base of the live crown.

We therefore applied an alternative approach to indicate crown length for spruce trees. Under the assumption that the upper part of the crown is the most important one for photosynthetic production, the height of the maximum crown radius (*ht_maxcr*) can be used as an indicator of crown length. We also found that *ht_maxcr* was significantly correlated to field-measured *htcb*, albeit with an expected bias.

Crown volume has been calculated by calculating the volume for each 1-m height layer with the given moving average of median crown radius and summing up all volumes above and including *htcb*, or above and including *ht_maxcr*.
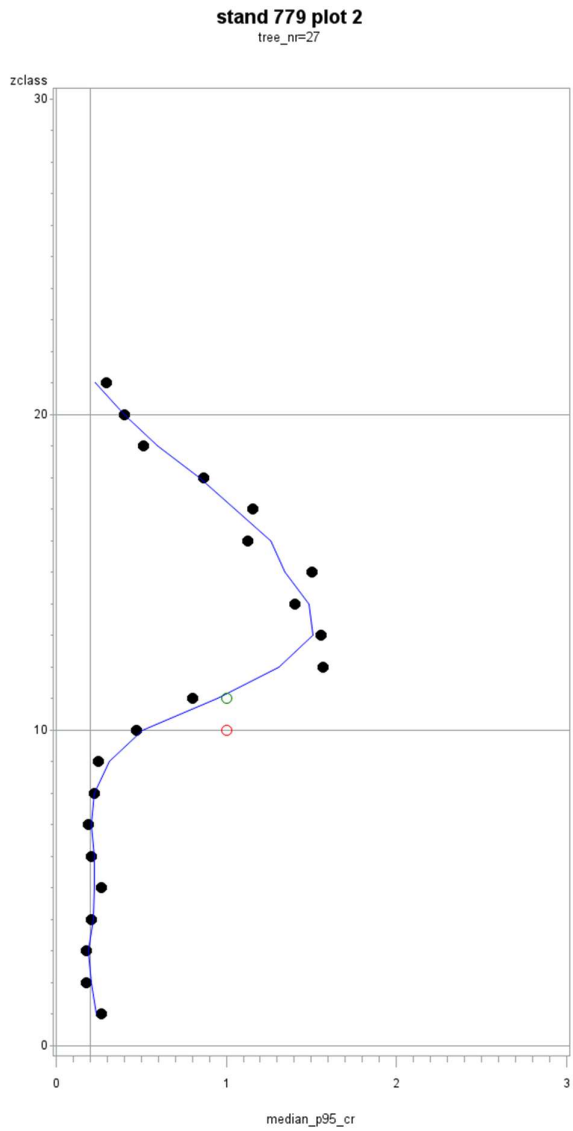
stand 779 plot 2
tree_nr=27

Figure 4. Voxel radius statistics indicating tree crown shape.
Black dots are median of 95-percentiles, blue line is the moving average of 3 neighboring height layers (zclass), green circle
is the automatically detected height of crown base, based on at least two successive recessions in crown radius of at least
10% of maximum crown radius or one recession of at least 20% (below height of maximum crown radius), red circle is
automatically detected height of crown base, based on a cumulative recessions in crown radius of at least 40% of maximum
crown radius (below height of maximum crown radius). Both axes are in meter.
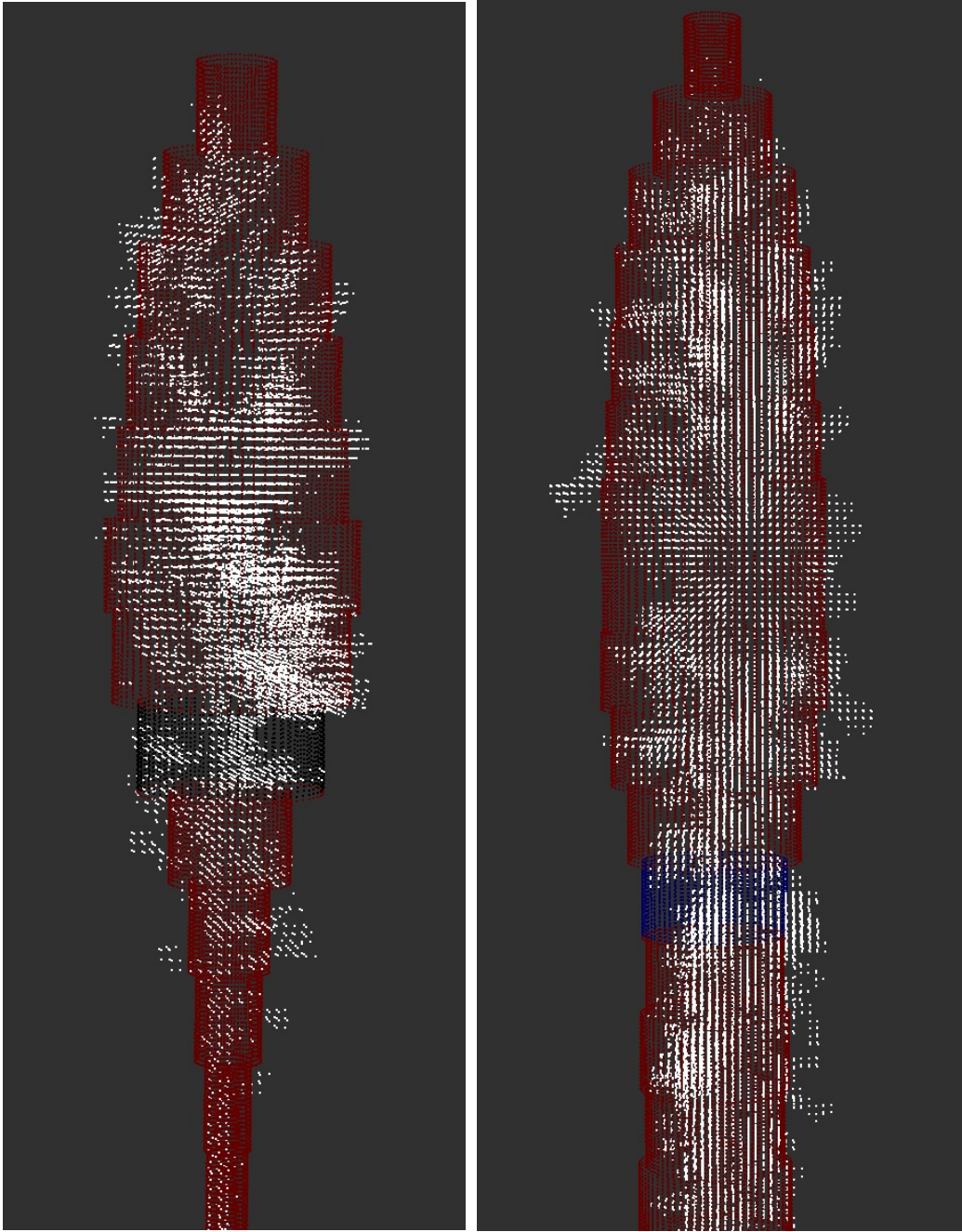
Figure 5. Rotational crown model (red) and tree voxel cloud (white).
Pine left, spruce right. Height layers in blue or black indicate the height to the crown base detected by our algorithm.
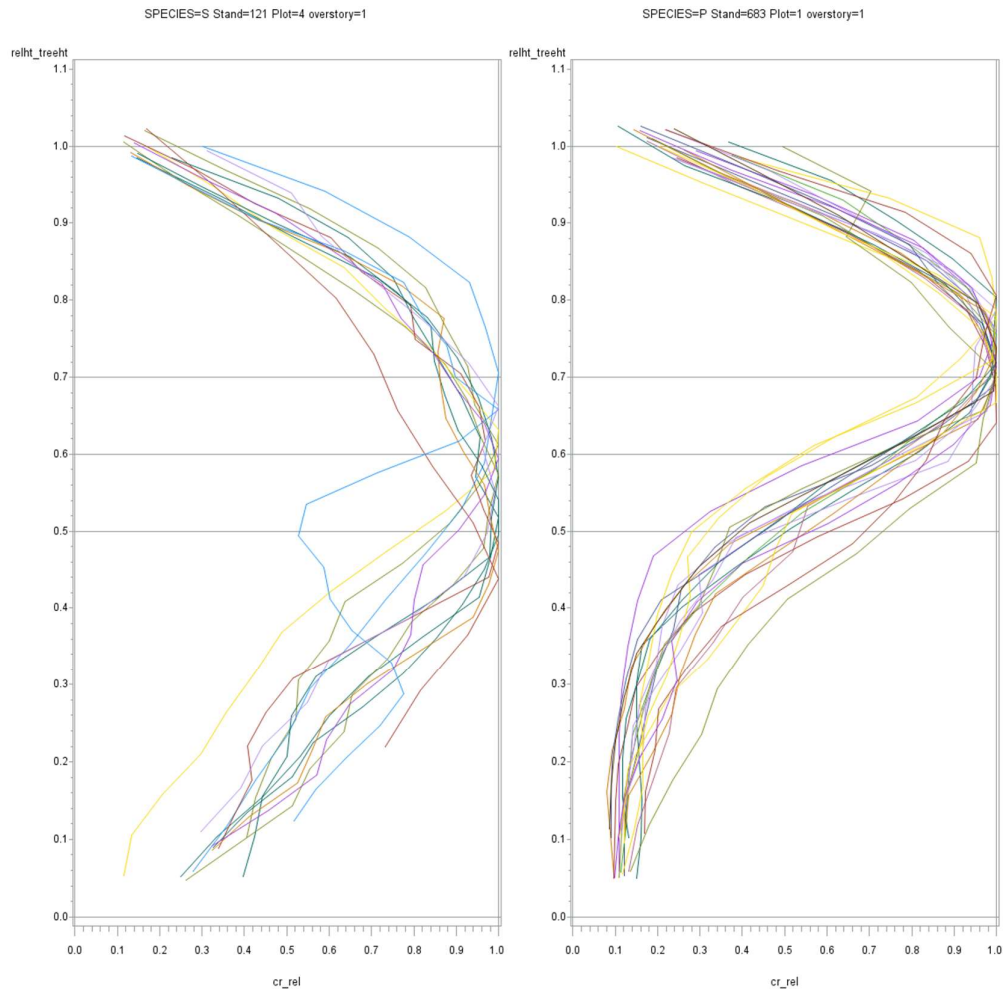
Figure 6. Two examples of MOVA crown models (Normalized to tree height and max. crown radius), illustrating a very similar crown shape of overstory trees (>12 cm dbh), irrespective of tree size. Spruce has longer crowns than pine.
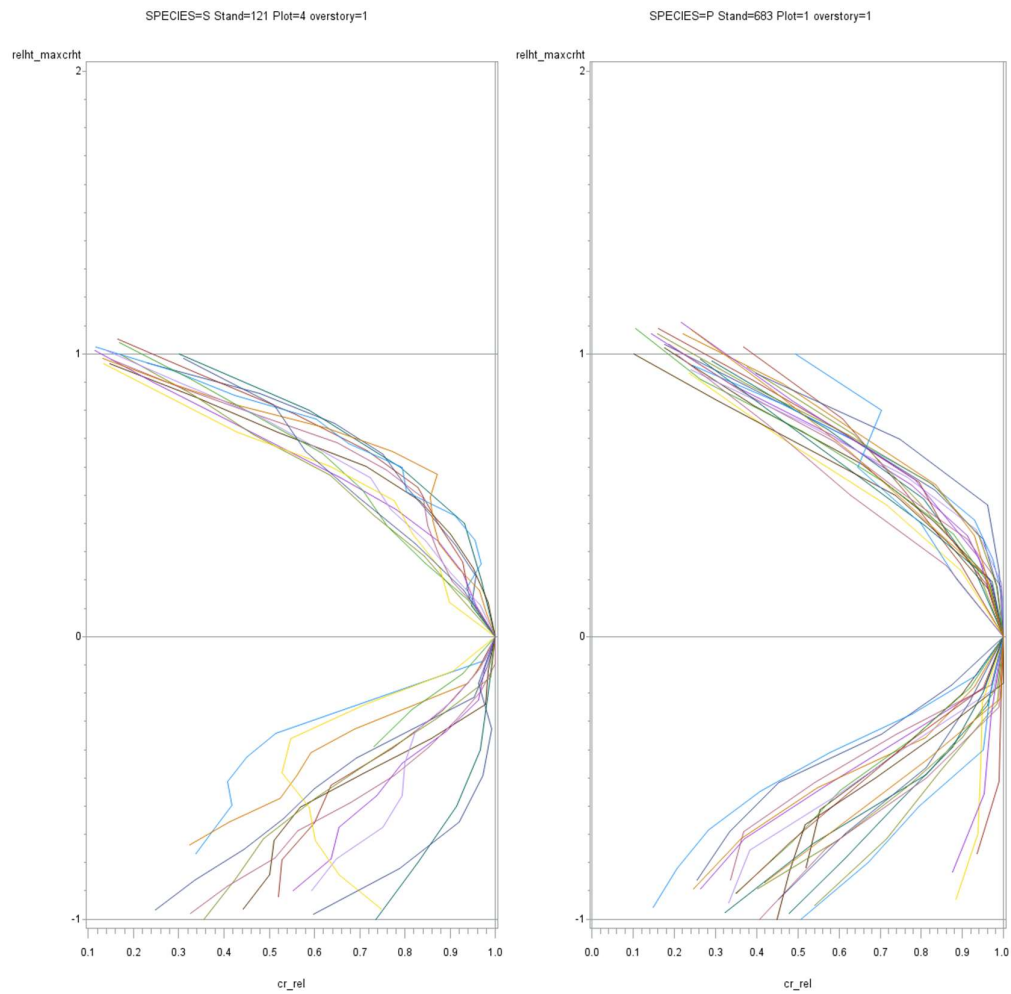
Figure 7. Two examples of MOVA crown models (Normalized to crown length (defined as tree height – height of max. crown radius) and max. crown radius), illustrating a very similar crown shape of overstory trees (>12 cm dbh), irrespective of tree size. Spruce has longer crowns than pine.

5. Analyses of crown variables for mixture effects

Dependent variables

- Maximum crown radius
- Crown length: *htcb* for pine, *ht_crmax* for spruce and pine
- Crown volume: above *htcb* for pine, above *ht_crmax* for spruce and pine

Independent variables

Tree dbh and/or height explained much of the variation in crown size variables.

 [Neighborhood_spec_comp.sas]

Tree-specific species proportion and competition indices used in this study define neighbors as trees within 4-m distance from the subject tree (no edge correction needed for trees in the core plot with 9 m radius).

Tree specific species proportion is the basal area of spruce in the total basal area of the neighborhood (in %).

The competition index is the basal area sum of all neighbors registered as living in 2017. To describe the competitive situation before the thinning, basal area of all trees and stumps were reconstructed to that point in time, using the following methods: for living trees the dbh was reduced to 90% (final version: based on 2 increment cores taken from each tree on the core plot, ring width after thinning was measured and average ring width substracted from dbh in 2017), for dead trees the dbh measured in 2017 was used (assuming that the tree was living at the time of thinning and died shortly after), and for stumps dbh before thinning was estimated from diameter of the stump under bark based on species-specific regressions fitted to a sample of living trees where diameter above bark has been measured at breast height and stump height in 2017 (N = 106 for pine, N = 173 for spruce), bark thickness was added based on species-specific regressions of dbh over bark in relation to dbh under bark, derived from bark thickness measurements on all trees on the core plot (N = 258 for pine, N = 530 for spruce).

Multiple regression models

Additive, interactions, log-transformations for crown volume

6. Acknowledgements

7. Literature

Barbeito, I., M. Dassot, D. Bayer, C. Collet, L. Drossler, M. Lof, M. del Rio, R. Ruiz-Peinado, D. I. Forrester, A. Bravo-Oviedo and H. Pretzsch (2017). "Terrestrial laser scanning reveals differences in crown structure of Fagus sylvatica in mixed vs. pure European forests." <u>Forest Ecology and Management</u> **405**: 381-390.

Gizachew, B., A. Brunner and B.-H. Øyen (2012). "Stand responses to initial spacing in Norway spruce plantations in Norway." <u>Scandinavian Journal of Forest Research</u> **27**(7): 637 - 648.

Hynynen, J., J. Repola and K. Mielikainen (2011). "The effects of species mixture on the growth and yield of mid-rotation mixed stands of Scots pine and silver birch." <u>Forest Ecology and Management</u> **262**(7): 1174-1183.

Makinen, H., A. Isomaki and T. Hongisto (2006). "Effect of half-systematic and systematic thinning on the increment of Scots pine and Norway spruce in Finland." <u>Forestry</u> **79**(1): 103-121.

Pretzsch, H., P. Biber and J. Dursky (2002). "The single tree-based stand simulator SILVA: construction, application and evaluation." <u>Forest Ecology and Management</u> **162**(1): 3-21.

Purves, D. W., J. W. Lichstein and S. W. Pacala (2007). "Crown plasticity and competition for canopy space: a new spatially implicit model parametrized for 250 North American tree species." <u>PLOS ONE</u> **9**: 1-11.

Raumonen, P., M. Kaasalainen, M. Akerblom, S. Kaasalainen, H. Kaartinen, M. Vastaranta, M. Holopainen, M. Disney and P. Lewis (2013). "Fast Automatic Precision Tree Models from Terrestrial Laser Scanner Data." <u>Remote Sensing</u> **5**(2): 491-520.

Tao, S. L., F. F. Wu, Q. H. Guo, Y. C. Wang, W. K. Li, B. L. Xue, X. Y. Hu, P. Li, D. Tian, C. Li, H. Yao, Y. M. Li, G. C. Xu and J. Y. Fang (2015). "Segmenting tree crowns from terrestrial and mobile LiDAR data by exploring ecological theories." <u>Isprs Journal of Photogrammetry and Remote Sensing</u> **110**: 66-76.

Trochta, J., M. Krucek, T. Vrska and K. Kral (2017). "3D Forest: An application for descriptions of three-dimensional forest structures using terrestrial LiDAR." <u>Plos One</u> **12**(5).